A

Dissertation

on

Synthesis and Photoluminescent Studies of SrY_2O_4: Eu/Ti Phosphors

Submitted in partial fulfilment of the requirement for the award of the degree of

MASTER OF SCIENCE
(M.Sc.)
in
Physics

(2019-2021)

Submitted by

Smriti

(301904017)

under the supervision of

Dr. O. P. Pandey
(Senior Professor, Head)

School of Physics and Materials Science
Thapar Institute of Engineering & Technology (TIET),
Patiala – 147004
June, 2021

CERTIFICATE

This is to certify that this dissertation entitled, **"Synthesis and Photoluminescent Studies of SrY_2O_4:Eu/Ti Phosphors"**, is submitted by Ms. Smriti (301904017) in fulfilment of requirement for the award of degree of Master of Science in Physics from School of Physics and Materials Science, Thapar Institute of Engineering & Technology, Patiala, India. It is an exclusive record of candidate's own research work under the guidance and supervision of **Dr. O.P. Pandey**. The dissertation has not been submitted in any other university or institute for the award of any other degree.

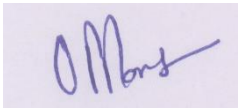

Dr. O.P. Pandey
Senior Professor, Head
School of Physics and Materials Science
Thapar Institute of Engineering & Technology
Patiala, India-147004

DECLARATION

I hereby declare that the work presented in this thesis report entitled, **"Synthesis and Photoluminescent Studies of SrY_2O_4: Eu/Ti Phosphors"**, by me in partial fulfilment of requirement for the award of degree of Master of Science in Physics from School of Physics and Materials Science, Thapar Institute of Engineering & Technology, Patiala, is an authentic record of my own research work under the supervision of **Dr. O.P. Pandey**, Senior Professor, Head of Department, School of Physics and Materials Science, Thapar Institute of Engineering & Technology, Patiala. The dissertation has not been submitted in any other university or institute for the award of any other degree.

Smriti

Regd. No: 301904017

ACKNOWLEDGEMENT

It is my utmost honour to pen down thanksgiving words for the individuals whom I met in the journey of dissertation compilation. I am privileged that I could embrace a wonderful research experience in their guidance. My foremost thank goes to my Masters' dissertation thesis supervisor ***Dr. O.P. Pandey*** (Senior Professor & Head), School of Physics and Materials Science, Thapar Institute of Engineering & Technology, Patiala, India. I am highly grateful to him that I could conduct my research work under his supreme research guidance. I am thankful to him for providing an environment where I could pursue my work without any interruption. This dissertation would not have been possible without his constant support and words of encouragement. I thank him for his thoughtful feedback that helped me understand the intricate matters.

I acknowledge my sincere gratitude to ***Prof. Prakash Gopalan***, Director and ***Staff Members*** of School of Physics and Materials Science, Thapar Institute of Engineering & Technology, Patiala for providing all necessary facilities for my research work.

I am highly grateful to ***Ms. Ruby Priya*** for her sincere guidance, scholarly advice and whole-heartedly willingness to help which made it possible to work on the topic of my dissertation. I thank her for embarking on this journey with me and staying with me till the end. This work would not materialize without her suggestions and inspiration. I would like to express my gratitude towards all my fellow labmates, ***Dr. Rameez Ahmad Mir***, ***Mr. Piyush Sharma***, ***Ms. Damandeep Kaur, Mr. Sanjay Upadhaya, Mr. Puneet Sharma***, and ***Ms. Sandeep Kaur*** for their invaluable help during the dissertation work.

I would like to thank my dear friends ***Navneet***, ***Anurag***, ***Kudrat*** and ***Navpreet*** who were always there for me to cheer up when I was feeling low. I am highly obliged to your unconditional time and support whenever I needed. Thank you, *PALS!!*

I am sincerely and whole-heartily thankful to my parents ***Mr. Vijay Kumar*** and ***Mrs. Sushma Rani***, for their wise counsel, unconditional support, blessings, prayers and words of motivation.

My final words go equally to all the concerned persons who have helped me directly and indirectly to accomplish this research work. It is the kindness of these acknowledged persons that this thesis sees the light of the day.

Above all, I am highly thankful to the supreme **Almighty** for his blessings, mercy and giving me patience and courage to carry out this work.

Smriti

ABSTRACT

In the present era, the demand of optoelectronic and display devices has increased enormously. For this purpose, phosphors with desirable emission characteristics are synthesized at a larger scale. The rare-earth doped phosphors have attracted a great attention owing their better emission properties over the non-rare earth materials. In the quest of synthesizing phosphors with better emission properties, the present work reports the synthesis and photoluminescence features of europium (Eu) doped SrY_2O_4 phosphors. It is a red light emitting phosphors and finds potential applications in the field emission displays. A series of Eu doped (1 to 11 mol%) SrY_2O_4 are synthesized via solid-state method. The structural and photoluminescent properties are synthesized via X-ray diffraction (XRD), Fourier transform infrared (FTIR) spectroscopy and photoluminescence (PL) technique. The quenching mechanism and type of interactions involved are studied via applying Dexter and Blasse's theory. The photometric parameters are calculated via determining the CIE coordinates. Further, the SrY_2O_4:Eu samples are co-doped with titanium (Ti) to study its effect on the emission characteristics. All the results are discussed in detail.

List of Figures

Page No.

List of Tables

Page No.

Chapter 2

Chapter 5

Table of contents

CHAPTER 1
INTRODUCTION

1.1. Introduction

In recent years, nanosize materials have attracted gigantic attention of researchers owing to their unique structural, optical, chemical, and electrical properties as compared to their bulk counterparts. Nanophosphor is one such class of nanomaterials that has emerged as potential candidates in the light industry. Lately, it has been found that rare-earth (RE) doped nanomaterials are of great importance in the field of optoelectronics device applications. The rare-earth doped materials are used in light emitting diodes (LEDs), display devices, sensors, lasers, field emission displays, etc. [1-3]. This is due to the sharp, narrow and intense emission spectra originating from the f-d and f-f transitions in the rare-earth elements. The demand of these materials is increasing tremendously due to increased consumption of optical sources. Generally, the transition metal or rare-earth ions are often used as dopants in phosphors. The transitions in transition metal ions originate because of d orbital electrons, resulting in the broad spectra. In rare earth ions, it is because of presence of electrons in f orbitals, which result in the sharp, narrow and strong emission spectra. However, the f orbitals of the Re^{3+} ions are effectively shielded by completely filled 5s and 5p subshells. The narrow emission are also a consequence of this shielding effect [4]. These transitions resulting from the f orbitals are barely affected by the environment in the host lattice, thus contributing the use of rare earth ions in various optoelectronic applications. There are 17 rare-earth elements (Scandium, Yttrium, and Lanthanides). Some of the trivalent rare earth ions such as La^{3+}, Y^{3+}, Sc^{3+}, Lu^{3+} have $^1S_0$ ground state, as a result of which transitions in 4f configurations are not observed.

1.2. Phosphors

Phosphors are the materials that generate visible light upon interaction with different types of radiations such as ultraviolet, infrared radiations, X-rays, electron beam, etc. It is a Greek word that stands for ‘torch bearer’. Phosphors consist of a host material and a luminescent center also referred to as an activator ion as shown in **Fig. 1.1 (a)**. A brief description about the three main constituents of a phosphor is mentioned as follows:

(a) ***Host lattice:*** The selection of host lattice depends on many factors and the desired application of the phosphors. The host material can be nitrides, sulphides,

silicates, oxides, aluminates, etc. [5-8]. There are some basic requirements for a good host material. It should possess a stable crystal structure, chemically and thermally stable, low phonon energy, etc. [3,9,10]. For a good host lattice, the energy losses due to heat energy should be comparably less. The emissions in the host lattice without any dopant is a result of Schottky or Frankel defects. For example, ZnO and $ZnAl_2O_4$ are such materials in which luminescence is observed due to the presence of defects [11,12].

(b) ***Activator:*** The host lattice are generally doped with an intentionally added impurity element called activator. The activator ion is chosen on the basis of interaction with the host lattice. The use of transition metal and rare-earth ions have been widely encouraged as activators because of the transitions of f-f and f-d electrons. In the process of luminescence, the activator ions absorb the incident radiation and are stimulated to higher energy levels. These excited atoms return to the ground state with the occurrence of radiative and non-radiative emissions. These absorbed energy is converted into visible light resulting in radiative emission. Thus, only dopants/activators called emission centers result in luminescence. So for an emission of desired color for particular applications activator ion is chosen accordingly. For example, Gd_2O_3 doped with Eu gives strong red emission, whereas Y_2O_3 doped with Dy gives intense yellow emission [13,14]. Here, Eu and Dy are the activator ions.

(c) ***Sensitizer:*** In some phosphors, the absorbed energy via the activator is insufficient to generate enough luminescence, because of forbidden transitions, so another impurity ion called sensitizer is added for energy transfer [15]. The energy absorbed by the sensitizer is then transferred to the activator ions via different mechanisms such as cross relaxation process. Then activator ion again goes to excited state and comes back to its ground state causing emissions. For example, when Eu doped $CaAl_2O_4$ is co-doped with Nd than the luminescence intensity of the phosphors increases as a result of energy transfer from Nd ion [16]. Here, Eu and Nd are playing the role of activator and sensitizer,

respectively. **Fig. 1.1 (b) and (c)** illustrate the role of activator and sensitizer in luminescent materials.

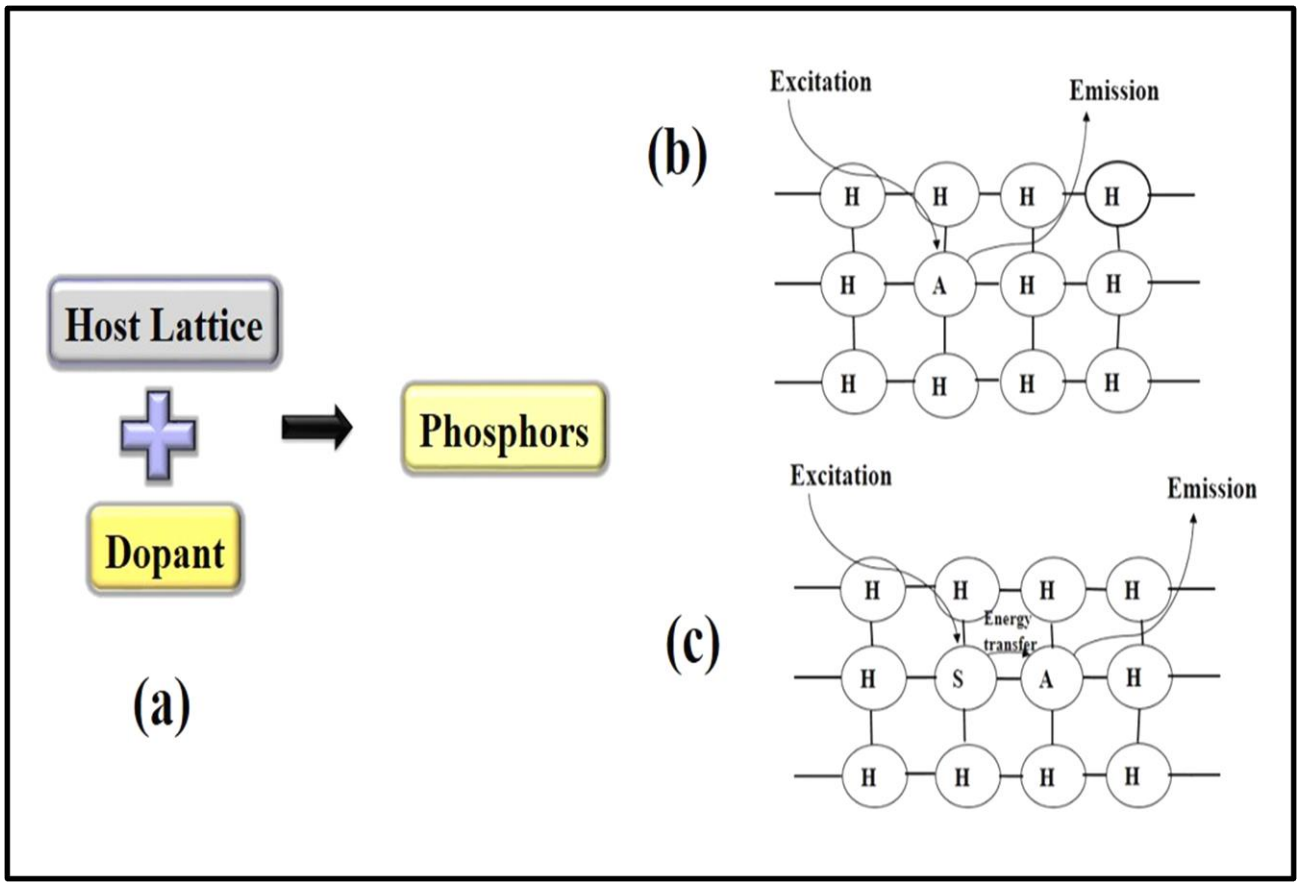

Figure 1.1: (a) Composition of a phosphor and **(b-c)** display luminescence phenomenon through energy transfer from sensitizer to activator [17].

1.3. Luminescence

The term luminescence comes from the Latin word called Lumen, which means light. This was introduced as 'luminescenz' by a German scientist named Eilhardt Wiedemann in 1888 [18]. Luminescence is the phenomenon of emission of light from a substance as a result of absorption of energy from an external source. This process occurs from electronically excited states [19]. The emitted light includes light in the visible region (400-750 nm) and near-ultraviolet and near-infrared region lying in close proximity of both the ends of the visible range. The gap between the lower and the higher energy states determines the frequency of the produced radiation. The phenomenon of luminescence by phosphors generally occurs in three ways that are up-conversion, down-conversion and down-shifting [20,21]. In up-conversion, the emission of a high energy photon of a shorter wavelength occurs by the absorption of two photons. In down

conversion phenomenon, two or more low energy photons are emitted by one high energy photon. Down shifting involves the conversion of a photon of higher energy to a photon of lower energy. The type of luminescence phenomenon depends on the choice of host and dopant.

1.4. Types of luminescence

There are many ways such as chemical reactions, energetic electrons, pressure on crystal, electric field etc. which stimulate the process of luminescence. Based upon the type of excitation source employed for excitation, luminescence can be categorized as follows:

I. ***Chemiluminescence-*** Chemical and electrochemical reactions cause this types of emission to occur.

II. ***Electroluminescence-*** An externally applied electromagnetic field results in the excitation of atoms and molecules of a substance. As a result of which, light is produced.

III. ***Bioluminescence-*** This phenomenon of light emission occurs as a consequence of Chemiluminescence in living organisms. For example fireflies produce light when luciferin, a chemical, produced by them reacts with oxygen.

IV. ***Cathodoluminescence-*** The emission takes place when electrons from an external source are bombarded on luminescent material, e.g. CRTs used to make displays.

V. ***Mechanoluminescence-*** It results from any mechanical impact upon a solid material. It may cause rupturing of bonds and can also result in elastic deformation of the material.

VI. ***Sonoluminescence-*** The emission takes place as short bursts of light when busting bubbles in fluid are energized by a sound.

VII. ***Thermoluminescence-*** It is a phenomenon when a crystalline material previously excited by ionizing radiation emits light upon heating. It is an important method for dating archaeological artifacts.

VIII. ***Photoluminescence-*** The absorption of photons causes the excitation of atoms and molecules in a substance. Based on the nature of excited state, photoluminescence is classified into two categories as described below:

a) ***Fluorescence:*** Fluorescence is a phenomenon in which emission of light takes place from a singlet excited state. The absorbed light is instantaneously emitted by the

substance. Also the light emission stops abruptly when the excitation source is removed.

b) ***Phosphorescence:*** In this phenomenon the emission of light takes place from a triplet energetic state. The absorbed light is not emitted instantaneously by the substance. The glow of phosphorescence lasts for several seconds after the elimination of excitation source. Afterglow is the term for this glow. The schematic mechanism of fluorescence and phosphorescence is shown in **Fig. 1.2**.

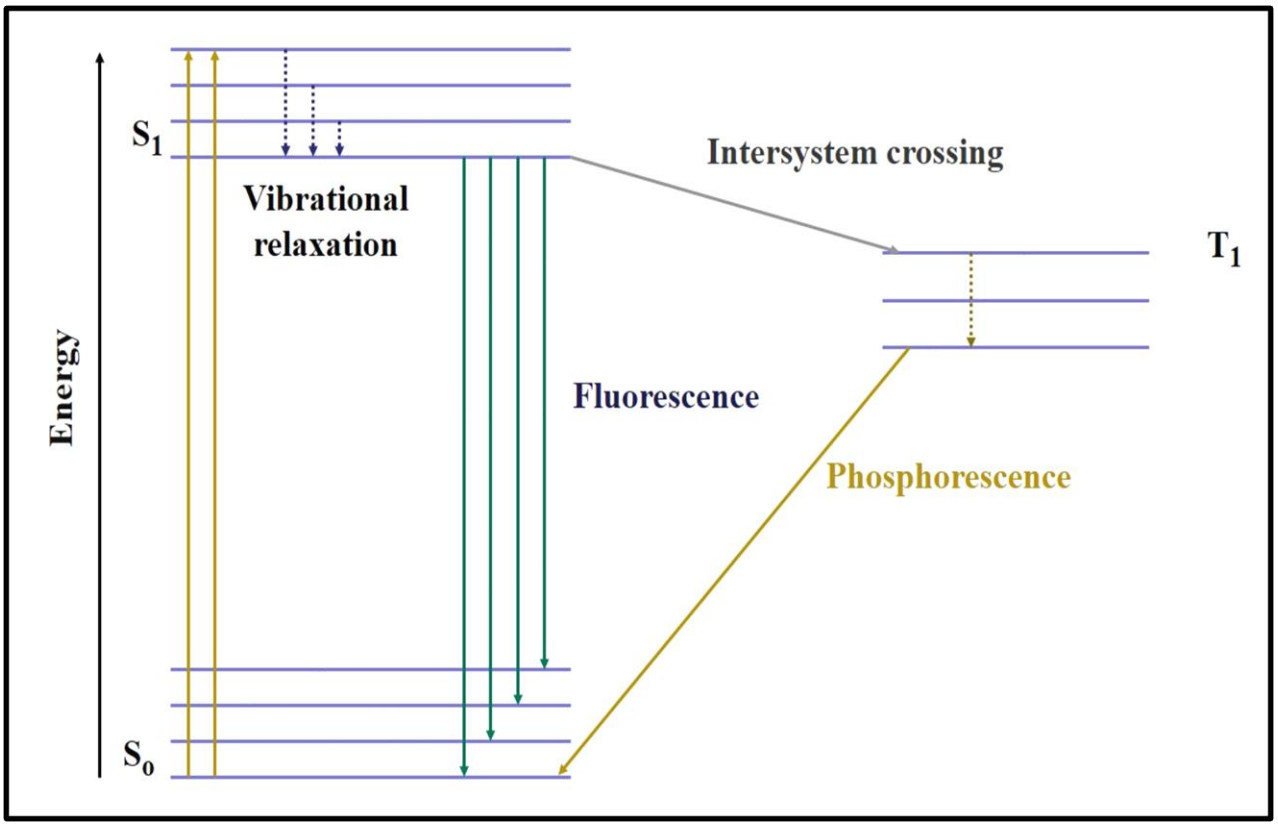

Figure 1.2: Fluorescence and phosphorescence mechanism in a substance [22]**.**

1.5. SrY_2O_4 (SYO) as host material

The selection of host material for phosphors is an important task. Good stability, better solubility and wide band gap are some of the significant characteristics of the host matrix. For this purpose, oxide based phosphors have been examined as potential options owing to their chemical and thermal stability, gas free emission, corrosion resistant properties, low phonon energy. Lately, many sulphide based phosphors have been used for commercial purposes like field emission displays (FEDs). These phosphors, on the other hand, are environmentally benign as they release hazardous sulphur gas and degrade when bombarded by an electron beam. A 'dead layer' is formed on the surface of the

optoelectronic device by the deposition of oxides and sulphates which are formed as a result of electron bombardment. This forbids the use of sulphide based phosphors in FEDs. On the contrary, oxide based phosphors are eco-friendly and are potential candidate for commercial applications like FEDs [15,23]. SrY_2O_4 (SYO) is one such oxide that has intrigued researchers for its use as a host matrix due to its unique thermal stability and also unique chemical, optical and magnetic properties [24,25]. It is an inter oxide of Y_2O_3 and SrO in pseudo binary phase diagram. The structure is composed of $Y_2O_4^{2-}$ framework with Sr^{2+} ions residing inside the framework. In this structure, the tetrahedral sites are occupied by half of the Y^{3+} ions and octahedral sites are occupied by remaining half of Y^{3+} ions and Sr^{2+} ions. Y^{3+} ions are surrounded by six oxygen atoms at both places and the Sr^{2+} ions are surrounded by eight oxygen atoms [26,27]. The dopant atom may substitute any of these two Y sites. Owing to its exceptional properties SYO has been widely used by researchers in many fields are shown in **Fig. 1.3**.

In recent times, the demand of field emission displays (FEDs) has increased enormously and has gained significant attention. Field emission display is a promising flat panel display technology that use field emission cathode as electron source. These electrons then strike the phosphor and produce coloured images. Thus, cathodoluminescence is a source of illumination in FEDs. In recent times, the demand of FEDs has increased enormously due to their less power consumption, quick response, excellent contrast ratio, high brightness, broad viewing angle and light weight. These FEDs are the future of flat panel display devices. For FEDs, phosphors are operated at high current densities (10-100 $\mu A\ cm^{-2}$) and low excitation voltage ($\leq$ 10 kV). Therefore, it is crucial to use phosphors which show good stability and high efficiency at a low voltage and a high current density and are chemically and thermally stable [28-30]. SYO is one of the promising host material and has been widely used in FEDs from the past few years. Its chemical and thermal stability, emission properties and environment friendly nature makes it a promising candidate for use in FEDs.

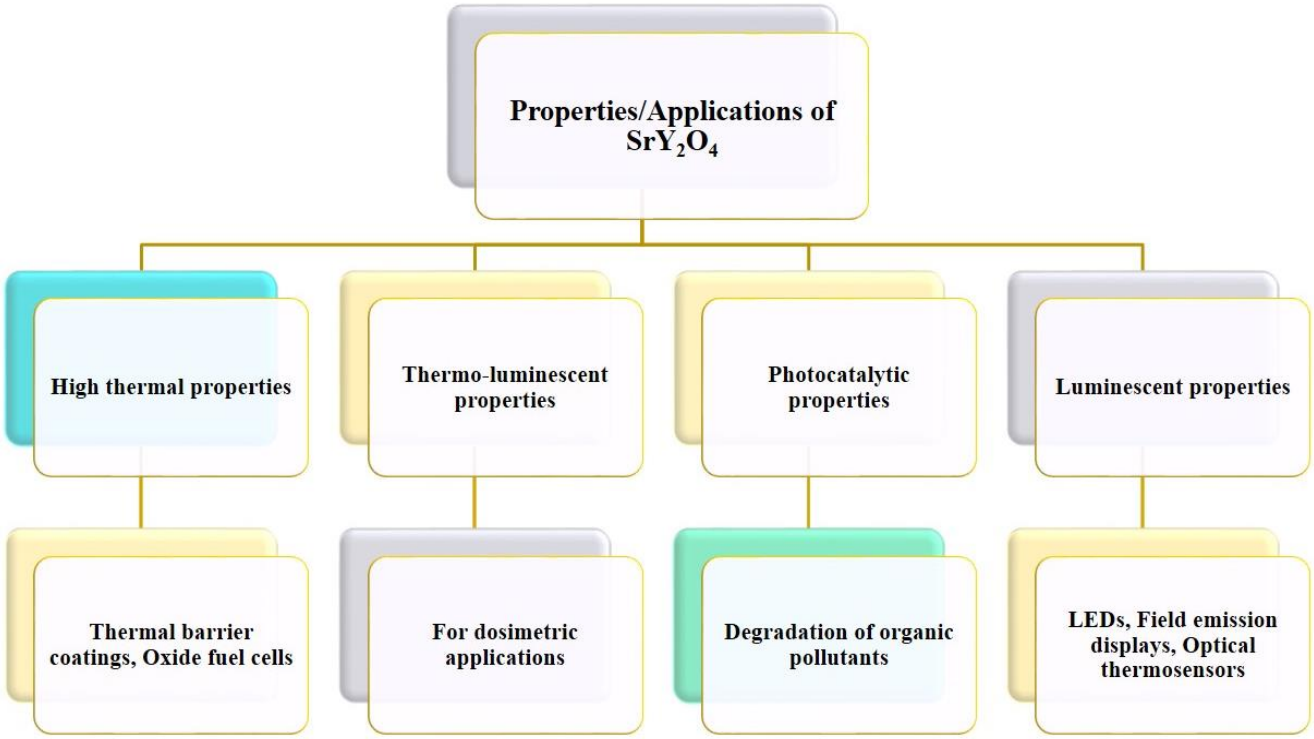

Figure 1.3: Various applications of SrY_2O_4.

1.6. SrY_2O_4 doped with Eu^{3+}

SrY_2O_4 is an efficient host matrix for the doping of many rare-earth ions due to similarity in ionic radii and valency. Till now, SYO doped with different rare-earth ions has been reported by various research groups. However, SYO is an ideal host matrix for the doping of europium (Eu) ions as the ionic radii of Y^{3+} (0.89 Å) and Eu^{3+} (0.95 Å) ions are close to each other [31]. Europium ions can replace any of these two Y^{3+} sites in SrY_2O_4 and influence the luminescence properties of the phosphors. SrY_2O_4 doped with Eu is a red light emitting phosphor under ultraviolet excitation. It exhibits sharp, narrow and intense emission spectra corresponding to $^5D_0 \rightarrow {}^7F_{J(J=0,1,2,3,4)}$ transitions of Eu^{3+} ions [32, 33]. In the chapter 2, synthesis of SrY_2O_4 by different synthesis routes and key findings by different researchers have been elaborated.

REFERENCES

1. Xiang G, Liu X, Xia Q, Jiang S, Zhou X, Li L, Jin Y, Ma L, Wang X, Zhang J, (2020) Deep-Tissue Temperature Sensing Realized in $BaY_2O_4:Yb^{3+}/Er^{3+}$with Ultrahigh Sensitivity and Extremely Intense Red Upconversion Luminescence. Inorg Chem 59:11054–11060.

2. Eladgham E.H, Demchenko D.O, Nakagawara T.A, Arachchige I.U, (2019), Facile synthesis of highly luminescent lithium silicate nanocrystals with varying crystal structures and morphology. CrystEngComm 21:1974–1983.

3. Pellerin M, Glais E, Lecuyer T, Xu J, Tanabe S.S, Richard C, (2018), $LaAlO_3:Cr^{3+}$, Sm^{3+}: Nano-perovskite with persistent luminescence for in vivo optical imaging. J Lumin 202:83–88.

4. Khan L.U, Zambon L.F.M, Santos J.L, Rodrigues R.V, Muraca D, Pirota K.R, Felinto M.C.F.C, Malta O.L, (2018), Red-emitting magnetic nanocomposites assembled from ag-decorated $Fe_3O_4@SiO_2$ and $Y_2O_3:Eu^{3+}$: Impact of iron-oxide/silver nanoparticles on Eu3+ emission. ChemistrySelect 3:1157–1167.

5. Vitola V, Millers D, Bite I, Smits K, Spustaka A, (2019), Recent progress in understanding the persistent luminescence in $SrAl_2O_4$:Eu,Dy. Material Sci Technol (United Kingdom) 35:1661–1677.

6. Huang Y, Zhou G, Wei D, Fan Z, Seo H.J, (2020), Phase-formation and luminescence properties of Eu^{3+}-doped Bi_2O_3 on synthetic process. J Lumin 220:116970.

7. Poort S.H.M, Reijnhoudt H.M, Van Der Kuip H.O.T, Blasse G, (1996) Luminescence of Eu^{2+} in silicate host lattices with alkaline earth ions in a row. J Alloys Compd 241:75–81.

8. Sebastian J.S, Swart H.C, Trottier T.A, Jones S.L, Holloway P.H, (1997), Degradation of ZnS field-emission display phosphors during electron-beam bombardment. J Vac Sci Technology A Vacuum, Surfaces, Film 15:2349–2353.

9. Portakal-Uçar Z.G, Oglakci M, Yüksel M, Can N, Ayacikli M, (2021), Structural and luminescence characterization of Ce^{3+} and Mn^{2+} co-activated zinc silicate nanocrystal obtained by gel combustion synthesis. Mater Res Bull 133:111025.

10. Priya R, Pandey O.P, Dhoble S.J, (2021) Review on the synthesis , structural and photo-physical properties of Gd_2O_3 phosphors for various luminescent applications. Opt Laser Technol 135:106663.

11. Jain M, Manju, Gundimeda A, Kumar S, Gupta G, Won S.O, Chae K.H, Vij A, Thakur A, (2019), Defect induced broadband visible to near-infrared luminescence in $ZnAl_2O_4$ nanocrystals. Appl Surf Sci 480:945–950.

12. Raji R, Gopchandran K.G, (2017), ZnO nanostructures with tunable visible luminescence: Effects of kinetics of chemical reduction and annealing. J Sci: Adv Material and Devices 2:51–58.

13. Bazzi R, Flores M.A, Louis C, (2004), Synthesis and properties of europium-based phosphors on the nanometer scale: Eu_2O_3, Gd_2O_3:Eu, and Y_2O_3:Eu. J Colloid Interface Science 273:191–197.

14. Atabaev T.S, Vu H.H.T, Kim H.K, Hwang Y.H, (2012), Synthesis and optical properties of Dy^{3+}-doped Y_2O_3 nanoparticles. J Korean Phys Soc 60:244–248.

15. Priya R, Kaur S, Sharma U, Pandey O.P, Dhoble S.J, (2020), A review on recent progress in rare earth and transition metals activated SrY_2O_4 phosphors. J. Mater. Sci. Mater. Electron. 31:13011–13027

16. Qu B, Zhang B, Wang L, Zhou R, Zeng X.C, (2015), Mechanistic study of the persistent luminescence of $CaAl_2O_4$:Eu,Nd. Chem Mater 27:2195–2202.

17. Halappa P, Shivakumara C, (2013), Synthesis and Characterization of Luminescent $La_2Zr_2O_7/Sm^{3+}$ Polymer Nanocomposites. Scrivener Publishing LLC 163–190

18. Valeur B, (2001), Introduction: On the Origin of the Terms Fluorescence, Phosphorescence, and Luminescence. 3–6.

19. Demchenko A.P ,(2009), Introduction to fluorescence. Introduction to Fluorescence Sensing 1–586.

20. Devi S, Khatkar A, Taxak V.B, Hooda A, Sehrawat P, Singh S, Khatkar S.P, (2020), Influence of Tb^{3+} doping on the structural and down-conversion luminescence behaviour of $SrLaAlO_4$ nanophosphor. J Lumin 221:117064.

21. Lin H, Yu T, Tsang M.K, Bai G, Zhang Q, Hao J, (2016), Near-infrared-to-near-infrared down-shifting and upconversion luminescence of KY_3F_{10} with single dopant of Nd^{3+} ion. Appl Phys Lett 108:1–5.

22. Lakowicz J.R, (1999), Principles of Fluorescence Spectroscopy (2006).

23. Holloway P.H, Trottier T.A, Sebastian J, Jones S, Zhang X.M, Bang J.S, Thomes W.J, Abrams B, (2000), Degradation of field emission display phosphors. J Appl Phys 88:483–488.

24. Manohar A, Krishnamoorthi C, (2017), Structural, optical, dielectric and magnetic properties of $CaFe_2O_4$ nanocrystals prepared by solvothermal reflux method. J Alloys Compd 722:818–827.

25. Kurosaki K, Tanaka T, Maekawa T, Yamanaka S, (2005), Thermal properties of polycrystalline sintered SrY_2O_4. J Alloys Compd 395:318–321.

26. Wang D, Wang Y, Wang L, (2007), Photoluminescence properties of $Sr(Y, Gd)_2O_4 : Eu^{3+}$ under VUV excitation. 126:135–138.

27. Lojpur V, Stojadinovi S, Mitri M, (2018), Effect of Eu^{3+} - Dopant Concentration on Structural and Luminescence Properties of SrY_2O_4 Nanocrystalline Phosphor and Potential Application in Dye-Sensitized Solar Cells. 50:347–355

28. Hirosaki N, Xie R.J, Inoue K, Sekiguchi T, Dieree B, (2007), Blue-emitting AlN: Eu^{2+} nitride phosphor for field emission displays. Appl Phys Lett 91:2–5.

29. Kamal C.S, Visweswara Rao T.K, Samuel T, Jasinski J.B, Ramakrishna Y, Rao M.C, (2017), Blue to magenta tunable luminescence from $LaGaO_3$: Bi^{3+}, Cr^{3+} doped phosphors for field emission display applications. RSC Adv 7:44915–44922.

30. Zhang Y, Geng D, Shang M, Zhang X, Li X, Cheng Z, Lian H, Lin J, (2013), Soft-chemical synthesis and tunable luminescence of Tb^{3+}, Tm^{3+}/Dy^{3+}-doped SrY_2O_4 phosphors for field emission displays. Dalt Trans 42:4799–4808.

31. Kolesnikov I.E, Povolotskiy A.V, Mamonova D.V. Manshina A.A, Mikhailov M.D, (2016), Photoluminescence properties of Eu^{3+} ions in yttrium oxide nanoparticles: Defect: Vs. Normal sites. RSC Adv 6:76533–76541.

32. Kolesnikov I.E, Kolokolov D.S, Kurochkin M.A, Voznesenskiy M.A., Osmolowsky M.G., Lahderanta E., Osmolovskaya, (2020), Morphology and doping concentration effect on the luminescence properties of SnO_2:Eu^{3+} nanoparticles. J Alloys Compd 822:153640.

33. Pavitra E, Seeta Rama Raju G, Park W, Yu J.S, (2014), Concentration and penetration depth dependent tunable emissions from Eu^{3+} co-doped SrY_2O_4:Dy^{3+} nanocrystalline phosphor. New J Chem 38:163–169.

CHAPTER 2
LITERATURE SURVEY

Un-doped and doped SrY_2O_4 (SYO) are synthesized via various synthesis routes. In this chapter, a peer-review survey of various synthesis routes of SYO has been done. The important findings of synthesis routes and their luminescent properties reported as of now by the researchers are discussed in the chronological order.

2.1 Literature survey of synthesis of SrY_2O_4

Yang *et al*. [1] in **2009** synthesized Yb^{3+}/Er^{3+} co-doped SrY_2O_4 nano crystalline phosphors via nitric decomposition method. XRD results revealed that all the peaks were indexed to orthogonal phase of SrY_2O_4 without any other impurity phase. The SEM images showed that the as prepared nano phosphors had sphere like particles with a diameter of about 1 μm. PL observations concluded that under 980 nm excitation red and green emissions were observed at 661 and 549 nm respectively.

Zhang and Wang [2] in **2010** prepared Eu^{3+} doped SrY_2O_4 nano crystalline phosphors synthesized via sol-gel and solid-state method. The photoluminescence spectra of the as synthesized samples was studied in vacuum ultraviolet and ultraviolet region. The morphologies of the products were determined by scanning electron microscopy (SEM) and X-ray diffraction method was employed to study the diffraction pattern. The excitation and emission bands monitored for the sample prepared by solid-state synthesis were found to be absent for the sample prepared using sol-gel synthesis. The phosphor doped with 2 mol% Eu resulted in maximum emission intensity at 147 nm excitation.

Zhang *et al.* [3] in **2012** synthesized rare-earth ions (Tb^{3+}, Eu^{3+}, Yb^{3+}, Tm^{3+}, Er^{3+}, and Ho^{3+}) doped SrR_2O_4 (R = Y and Gd) via solid-state method. The prepared samples were analyzed by photoluminescence spectra (PL) and X-Ray diffraction. It was noted that Tb^{3+}, Eu^{3+}, doped SrY_2O_4 resulted in green and red emissions respectively. Luminescence properties of Yb^{3+}, Tm^{3+}, Er^{3+}, and Ho^{3+} doped $SrGd_2O_4$ were also investigated. It was concluded that SrR_2O_4 are outstanding phosphors.

Dubey *et al.* [4] in 2013 synthesized Eu^{3+} doped SYO phosphor by solid-state reaction method. X-Ray diffraction (XRD), SEM and PL techniques were employed to characterize the as synthesized samples. The crystal structure of the samples was found to be orthorhombic. The excitation spectrum consisted of peaks at 247 and 364 nm and

the emission spectra consisted of peaks around 590, 612 and 624 nm. Thus the phosphors gave intense peak at red emission.

Pavitra *et al.* [5] in **2014** synthesized Dy^{3+} ion single-doped and Dy^{3+}/Eu^{3+} co-doped white light emitting SrY_2O_4 nano crystalline phosphors synthesized via sol-gel method. The crystalline phase was observed at 1300 ℃. X-Ray diffraction pattern confirmed the orthorhombic structure of the sample. The PL spectra of Dy^{3+} ion single-doped phosphors showed that the yellow emission band was more dominant than the blue emission band and the PL spectra of Dy^{3+}/Eu^{3+} co-doped SrY_2O_4 samples exhibited warm white light emission. The samples were found out to be promising materials to obtain natural white light for optical display systems and indoor applications.

Pavitra *et al.* [6] in **2014** prepared $Er^{3+}/Tm^{3+}/Yb^{3+}$ ions tri-doped SrY_2O_4 nano phosphors via sol-gel method. The pure orthorhombic structure was confirmed by XRD patterns and the particles were found to have spherical morphology. A bright green emission around 551 nm was observed in Er^{3+} ions single-doped phosphors. The intensity of the red emission band around 664 nm was improved by co-doping of Yb^{3+} with Er^{3+} ions in the host matrix. This resulted in a greenish yellow emission under 980 nm excitation. White light emission was observed in the tri-doped SrY_2O_4.

Singh *et al.* [7] in **2015** synthesized europium doped MY_2O_4 (M=Mg, Ca, Sr) via combustion route. It was observed that the photoluminescence properties of these Eu^{3+} activated oxides exhibited red luminescence. The structural and morphological studies were conducted by the analysis of X-ray diffraction pattern, scanning electron microscopy (SEM), and transmission electron microscopy (TEM) micrographs. The emission intensity of SYO:Eu^{3+} was found to be maximum among the other samples.

Opravil *et al.* [8] in **2016** prepared SrY_2O_4 samples using solid-state method. The reaction of SrO with equimolar amount of Y_2O_3 resulted in the synthesis of these phosphors. The properties and the behaviour during the reaction of SrY_2O_4 powders with water were investigated in order to evaluate the properties, to explain the hydration process and to identify the synthesized products.

Xianlang *et al.* [9] in 2016 synthesized Er^{3+}/ Yb^{3+} co-doped SrY_2O_4 phosphors using $SrCO_3$ and Y_2CO_3 as initial precursors by solid-state reaction method. Luminescence spectrum studies showed that the main red peaks and the minor green peaks of up-conversion emissions were located at approximately 634-681 nm and 543–570 nm,

respectively. It was found that the emission color of the proposed phosphors could be successfully modulated by the joint contributions of altered Yb^{3+} composition and excitation power.

Tamarkar and Upadhayay [10] in **2017** prepared Tb^{3+} doped SrY_2O_4 phosphors using solution combustion synthesis route. The structure of the prepared phosphor was determined by using X-ray diffraction technique and morphology by the field emission scanning electron microscopy (FESEM). Under 254 nm ultra violet excitation, the phosphor exhibited an intense green emission around 543 nm. The sample was also used to prepare efficient green LEDs. Also the phosphor was found to be useful for sensing applications such as biological and chemical sensing.

Taikar [11] in **2018** synthesized SYO from $SrCO_3$ and Y_2O_3 using combustion route. The as-synthesized phosphors were activated with Eu^{3+}, Tb^{3+}, Sm^{3+}, Ce^{3+} and Bi^{3+} as dopants. The samples were characterized by photoluminescence technique. The emission wavelengths of SYO activated with Eu^{3+}, Tb^{3+}, Sm^{3+}, Ce^{3+} and Bi^{3+} were found around 611, 553, 610, 460 and 420 nm, respectively. The prepared phosphors were found to be very useful in display devices and related applications.

Shaik *et al.* [12] in **2018** carried out photoluminescence investigations on Eu^{3+} doped Strontium Yttrium oxide (SYO) nano phosphors synthesized via polyol method. The as-prepared samples were analysed by XRD and photoluminescence techniques for the identification of phase and luminescence properties. The emissions were observed at 615 nm under excitation at 255 nm for Eu^{3+} doped SYO nano phosphors. The synthesized SrY_2O_4: Eu^{3+} nano phosphors were found to be a suitable material for field emission display and LED applications.

Wei *et al.* [13] in **2018** synthesized SrY_2O_4:Bi^{3+}, Eu^{3+} using conventional solid-state method. X-ray diffraction, excitation and emission spectra, decay curves as well as temperature-dependent luminescence were applied to characterize the as-obtained phosphors. Under ultraviolet (UV) excitation, blue luminescence centered at 410 nm was found in SYO:Bi^{3+} phosphors. By altering Eu^{3+} content, tunable emission from blue to red was realized. These results indicated that this kind of easy fabrication, low-cost and highly stable SYO:Bi^{3+}, Eu^{3+} are potential candidates for blue-red phosphors for application in UV chip based w-LEDs.

Ghorpade *et al.* [14] in **2020** prepared Dy^{3+}:SrY_2O_4 nanophosphors via solution combustion method using glycine as an organic fuel. The as-prepared samples were characterized by XRD, FESEM, HRTEM and Fourier transform infrared spectroscopy (FTIR). FESEM micrographs showed spherical particles and closely crowded morphology. The samples were found to be suitable for photocatalytic degradation of Rhodamine-B dye under UV light treatment. Also PL emission spectra revealed broad intense blue and yellow emission peaks at an excitation wavelength of 354 nm.

Ghorpade *et al.* [15] in **2020** prepared Eu^{3+} doped SrY_2O_4 nanophosphors via solution combustion method. The samples were characterized by XRD, FESEM, high-resolution transmission electron microscopy (HR-TEM), UV-Vis spectroscopy and PL techniques to know about the structural, morphological and spectroscopic properties. FESEM micrographs revealed that nearly spherical and agglomerated particles were formed. A strong red emission at 613 nm was found at excitation wavelength of 254 nm. The analysis revealed that the as prepared phosphors would be used as red color emitting phosphors in W-LEDs and FEDs.

Singh *et al.* [16] in **2020** synthesized Gd^{3+} ion activated SrY_2O_4 phosphors using sol-gel method. XRD patterns revealed that the orthorhombic phase of SrY_2O_4 could be obtained by this method. The photoluminescence spectra were recorded to understand the luminescence behaviour of the as-prepared phosphors. The phosphors exhibited two emission bands, one at 309 nm and other at 315 nm upon excitation of 275 nm. The PL spectra allowed them to consider the prepared phosphor as a potential candidate for application in phototherapy lamps.

Based on the literature survey, the outcomes of various research papers including synthesis method, excitation and emission wavelengths, precursors and morphology are summarised in chronological order in **Table 2.1**.

Table 2.1: Summary of various synthesis routes and luminescent characteristics of SrY_2O_4 phosphors.

SrY_2O_4: Dopant	**Synthesis route**	**Precursors**	**Excitation wavelength**	**Emission wavelength**	**Synthesis temp. (duration)**	**Morphology**	**Ref.**
SrY_2O_4: Yb^{3+}/Er^{3+}	Nitric decomposition method	$SrCO_3$, Y_2O_3, Yb_2O_3, Er_2O_3, Nitric acid	980 nm	549 nm 661 nm	1200 °C (10h)	Sphere-like	[1]
SrY_2O_4: Eu^{3+}	Sol-gel and Solid-state method	$SrCO_3$, Y_2O_3, Eu_2O_3	242 nm 265 nm	616 nm 610 nm	1300 °C (7h)	Highly aggregated particles	[2]
SrR_2O_4: $Tb^{3+}/Eu^{3+}/Yb^{3+}/Tm^{3+}/Er^{3+}/Ho^{3+}$ (R= Y, Gd)	Solid-state method	$SrCO_3$, Y_2O_3, Eu_2O_3, Gd_2O_3, Er_2O_3, Tb_4O_7, Yb_2O_3, Tm_2O_3, Ho_2O_3	230 nm	611 nm	1300 °C (7h)	-	[3]
SrY_2O_4: Eu^{3+}	Solid-state method	$SrCO_3$, Y_2O_3, Eu_2O_3	400 nm	613 nm	1350 °C (3h)	-	[4]
SrY_2O_4: Dy^{3+}/Eu^{3+}	Sol-gel method	$Sr(NO_3)_2$, $Y(NO_3)_3.6H_2O$, $Dy(NO_3)_3.5H_2O$,$Eu(NO_3)_3.5H_2O$	351 nm	578 nm	500 °C (5 h)	Closely packed with single crystalline structure	[5]
SrY_2O_4: $Er^{3+}/Tm^{3+}/Yb^{3+}$	Sol-gel method	$Sr(NO_3)_2$, $Y(NO_3)_3.6H_2O$, $Dy(NO_3)_3.5H_2O$,$Er(NO_3)_3.5H_2O$, $Tm(NO_3)_3.5H_2O$, $Yb(NO_3)_3.5H_2O$	980 nm	551 nm	500 °C (5 h)	Nearly Spherical	[6]
MY_2O_4 (M=Mg, Ca, Sr):Eu^{3+}	Combustion synthesis	$M(NO_3)_2.xH_2O$, $Y(NO_3)_3.6H_2O$, $Eu(NO_3)_3.5H_2O$	267 nm	612 nm	1100 °C (1h)	Spherical particles	[7]
SrY_2O_4	Solid-state synthesis	$SrCO_3$, Y_2O_3	-	-	1650 °C (1h)	-	[8]
SrY_2O_4: Er^{3+}/ Yb^{3+}	Solid-state synthesis	$SrCO_3$, Y_2O_3, Er_2O_3, Yb_2O_3	1550 nm	552 nm	1350 °C (3h)	-	[9]

SrY_2O_4: Tb^{3+}	Combustion synthesis	$Sr(NO_3)_2$, $Y(NO_3)_3$.6 H_2O, $Tb(NO_3)_3$.5 H_2O	254 nm	543 nm	900 °C (2 h)	Agglomerated particles	[10]
SrY_2O_4: Eu^{3+}, Tb^{3+}, Sm^{3+}, Ce^{3+} and Bi^{3+}	Combustion synthesis	$SrCO_3$, Y_2O_3	253 nm 295 nm 409 nm 345 nm 330 nm	611 nm 553 nm 610 nm 460 nm 420 nm	1000 °C (3h)	-	[11]
SrY_2O_4:Eu^{3+}	Polyol method	$Sr(NO_3)_2$, $Y(NO_3)_3$·6 H_2O, $Eu(NO_3)_2$	255 nm	615 nm	1000 °C (5h)	-	[12]
SrY_2O_4:Bi^{3+}, Eu^{3+}	Solid-state method	$SrCO_3$, Y_2O_3, Eu_2O_3, Bi_2O_3	410 nm	611 nm	1200 °C (10 h)	-	[13]
SrY_2O_4:Dy^{3+}	Combustion synthesis	$Sr(NO_3)_2$, $Y(NO_3)_3$·6 H_2O, $Dy(NO_3)_3$· $6H_2O$	354 nm	581 nm	1300 °C (3h)	Nearly spherical	[14]
SrY_2O_4:Eu^{3+}	Combustion synthesis	$Sr(NO_3)_2$, $Y(NO_3)_3$·6 H_2O, $Eu(NO_3)_3$·5 H_2O	254 nm	613 nm	1300 °C	Nearly spherical	[15]
SrY_2O_4:Gd^{3+}	Sol-gel synthesis	$Sr(NO_3)_2$, $Y(NO_3)_3$·6 H_2O, $Gd(NO_3)_3$· $6H_2O$	275 nm	315 nm	1000 °C (3h)	Agglomerates of varying shape	[16]

REFERENCES

1. Yang J, Xiao S, Ding J, Yang X, Wang X, (2009), Preparation and photoluminescence properties of $SrY_2O_4:Yb^{3+}$, Er^{3+} powders. J Alloys Compd 474:424–427.

2. Zhang J, Wang Y, (2010), Luminescence of $SrY_2O_4:Eu^{3+}$ associated with defects. J Mater Res 25:2120–2124.

3. Zhang J, Wang Y, Guo L, Huang Y, (2012), Vacuum ultraviolet-ultraviolet, x-ray, and near-infrared excited luminescence properties of SrR_2O_4: RE^{3+} (R = y and Gd; RE = Tb, Eu, Yb, Tm, Er, and Ho). J Am Ceram Soc 95:243–249.

4. Dubey V, Kaur J, Agrawal S, Suryanarayana N.S, (2013), Synthesis and characterization of Eu^{3+} doped SrY_2O_4 phosphor. Optik (Stuttg) 124:5585–5587.

5. Pavitra E, Seeta Rama Raju G, Park W, Yu J.S, (2014), Concentration and penetration depth dependent tunable emissions from Eu^{3+} co-doped $SrY_2O_4:Dy^{3+}$ nanocrystalline phosphor. New J Chem 38:163–169.

6. Pavitra E, Seeta Rama Raju G, Oh J.H, Yu J.S, (2014), Pump power induced tunable upconversion emissions from $Er^{3+}/Tm^{3+}/Yb^{3+}$ ions tri-doped SrY_2O_4 nanocrystalline phosphors. New J Chem 38:3413–3420.

7. Singh D, Tanwar V, Bhagwan S, Nishal V, Sheoran S, Kadyan S, Kadyan P, (2015), Synthesis and Optical Characterization of Europium Doped MY_2O_4 (M = Mg, Ca, and Sr) Nanophosphors for Solid State Lightening Applications . Indian J Mater Sci 2015:1–8.

8. Opravil T, Ptáček P, Šoukal F, Bartoníčková E, Wasserbauer J, (2016), Solid-state synthesis of SrY_2O_4 and $SrSm_2O_4$: Mechanism and kinetics of synthesis, reactivity with water and thermal stability of products. J Therm Anal Calorim 123:181–194.

9. Shen X, Xing M, Tian Y, Fu Y, Peng Y, Luo X, (2016), Upconversion photoluminescence properties of $SrY_2O_4:Er^{3+},Yb^{3+}$ under 1550 and 980 nm excitation. J Rare Earths 34:458–463.

10. Tamrakar R.K, Upadhyay K, (2018), Combustion Synthesis and Luminescence Behaviour of the Tb^{3+} Doped SrY_2O_4 Phosphor. J Electron Mater 47:651–654.

11. Taikar D.R, (2018), Synthesis and luminescence property of $SrY_2O_4:M$ ($M = Eu^{3+}$, Tb^{3+}, Sm^{3+}, Ce^{3+}, Bi^{3+}) phosphors. J Lumin 204:24–29.

12. Shaik E.B, Rajyalakshmi S, Dharmaja M.S.S, Sangeetha B, Lakshmi R, Krishna Y, (2018), The effect of Eu^{3+} on SrY_2O_4 nano phosphors. AIP Conf Proc 1992:3–7.

13. Wei R, Zheng Z, Shi Y, Peng X, Wang H, Tian X, Hu F, Guo H, (2018), Tunable emission with excellent thermal stability in single-phased $SrY_2O_4:Bi^{3+}$, Eu^{3+} phosphors for UV-LEDs. J Alloys Compd 767:403–408.

14. Ghorpade S.P, Kottam N, Melavanki R, Patil N.R, (2020), Photoluminescence, TGA/DSC and photocatalytic activity studies of Dy^{3+} doped SrY_2O_4 nanophosphors. RSC Adv 10:21049–21056.

15. Ghorpade S.P, Hari Krishna R, Melavanki R.M, (2020), Effect of Eu^{3+} on optical and energy bandgap of SrY_2O_4 nanophosphors for FED applications. Optik (Stuttg)

208:164533.

16. Singh V, Swapna K, Kaur S, Rao A.S, Rao J.L, (2020), Narrow-Band UVB-Emitting Gd-Doped SrY_2O_4 Phosphors. J Electron Mater 49:3025–3030.

CHAPTER 3
MOTIVATION AND OBJECTIVES

3.1. Motivation

The emission properties of the host matrix are influenced by a variety of factors such as type of crystal structure, excitation wavelength, dopants and co-dopants. After peer-review of literature survey in ***Chapter 2***, it has been observed that solid-state method is an efficient method for the synthesis of SrY_2O_4 samples. Till now, many researchers have reported the synthesis and emission properties of the rare-earth doped SYO phosphors. However, the structural changes, bandgap variations, and decay curves are not studied in detail. In the present study, europium ions as a probe in SYO phosphors have been chosen to study aforementioned properties.

Furthermore, it is found that the incorporation of co-dopants in the host lattice significantly changes the optical properties. The co-dopants act as sensitizers and transfer their energy to enhance the photoluminescent characteristics via various mechanisms. Many rare-earth ions are used as sensitizers, but their high cost and less abundance make their limited applications in optoelectronic devices. Cui *et al*. [1] studied the effect of Ti^{4+} co-doping in $Y_2O_2S:Eu^{3+}$ phosphors synthesized via sol-gel technique. It was found that luminescent properties of the phosphor improved with changing the co-dopant concentrations. Sun *et al.* [2] synthesized $BaZrO_3$:Eu phosphor via solid-state reactions method and studied the effect of Ti^{4+} co-doping on its luminescent properties. It was concluded that Ti^{4+} co-doping is an effective way to enhance the performance of phosphors as the phosphors showed stronger afterglow, longer decay time as compared to $BaZrO_3$:Eu phosphors. Sudhakar *et al.* [3] also observed that Ti^{4+} co-doping enhanced the emission characteristics of lead arsenate glass system **(**$40PbO– (60-x)As_2O_3– xTiO_2$**)** doped with Pr^{3+}. With the incorporation of Ti^{4+} ions, the intensity of violet-blue emission of Pr^{3+} ions was amplified by nearly five times. Ryu and Bartwal [4] investigated photoluminescent properties of Ti^{4+} co-doped $CaAl_2O_4:Eu^{2+}$. The as-prepared phosphor was found to exhibit blue emission. With co-doping, the intensity increased and longer persistence luminescence was observed. Yang *et al.* [5] studied the effect of Ti^{4+} co-doping on Cr^{3+} doped $MAl_{12}O_{19}$ (M= Ca, Sr). The intensity of luminescence was enhanced dramatically with the addition of co-dopant. Thus, it is observed that the co-dopant in with titanium (Ti^{4+}) ions enhanced the luminescent properties of the various phosphors. Inspiring with such finding, we have taken titanium as co-dopant in the SYO:Eu system

to study various structural, optical and luminescent properties. To the best of our knowledge, there is no report on the co-doping of Ti^{4+} in the doped SYO phosphors. Thus, present study will add significant results in the existing literature.

3.2. Objectives

In the present research study, following objectives have been proposed to work on:

1. To synthesize phase pure SrY_2O_4 samples via solid-state method.
2. To study the effect of europium (Eu) ion doping in SrY_2O_4 samples.
3. To study the effect of co-doping of titanium (Ti) ions in the optimized Eu doped SYO sample. Here, optimized means the SYO sample for which maximum emission intensity is achieved when doped with particular concentration of europium.
4. To characterize the samples by various techniques such as X-Ray Diffraction (XRD), photoluminescence (PL) flourospectrometer, Fourier transform infrared spectrometer (FT-IR), UV-Visible spectrometer, and field emission scanning electron microscope (FESEM).

REFERENCES

1. Cui CE, Liu H, Huang P, Wang L, (2014), Influence of Mg^{2+}, Ti^{4+} co-doping concentration on the luminescence properties of $Y_2O_2S:Eu^{3+}$, Mg^{2+}, Ti^{4+} nanotube arrays. J Lumin 149:196–199.
2. Sun D, Li D, Zhu Z, Xiao J, Tao Z, Liu W, (2012), Photoluminescence properties of europium and titanium co-doped $BaZrO_3$ phosphors powders synthesized by the solid-state reaction method. Opt Mater (Amst) 34:1890–1896.
3. Sudhakar P, Kumar V.R, Kumar V.R, Purnachand N, Veeraiah N, (2018), Violet-blue emission characteristics of Pr^{3+} ions codoped with Ti^{4+} ions in lead arsenate glass system. J Lumin 199:416–422.
4. Ryu H, Bartwal K.S, (2008), Photoluminescent studies on Ti co-doped $CaAl_2O_4:Eu^{2+}$, Ti^{3+} phosphor. Phys B Condens Matter 403:1843–1847.
5. Yang H, Zhao W, Song E, Yun R, Huang H, Song J, Zhong J, Zhang H, Nie Z,Li Y, (2020), Highly flexible dual-mode anti-counterfeiting designs based on tunable multi-band emissions and afterglow from chromium-doped aluminates. J Mater Chem C 8:16533–16541.

CHAPTER 4
RESEARCH METHODOLOGY

4.1. Materials

Strontium carbonate (*Sigma Aldrich, 99%*) and yttrium oxide (*Sigma Aldrich, 99%*) were used to synthesize the SrY_2O_4 host lattice. Europium oxide (*Sigma Aldrich, 99%*) and titanium oxide (*Sigma Aldrich, 99%*) were used as precursors for doping and co-doping in SrY_2O_4. These reagents were of analytical grade and utilized in as received condition without further purification.

4.2. Synthesis Method

Un-doped, europium (Eu^{3+}) doped and titanium (Ti^{4+}) co-doped SrY_2O_4 phosphors were prepared via the conventional solid-state reaction method. For the preparation of undoped SrY_2O_4, the stoichiometric amounts of $SrCO_3$ and Y_2O_3 were thoroughly ground in an agate mortar for 1 h. These ground precursors were shifted to an alumina crucible, which was then placed at 1000 °C for 4 h in the high temperature muffle furnace. The furnace heating rate was maintained at 3 °C/min. After cooling of samples to room temperature, the samples were further ground for 30 min and further subjected to sintering at 1300 °C for 6 h. The pictorial representation of synthesis of un-doped SYO is shown in **Fig. 4.1**. Further, in another set of experiments europium was added as a dopant in SYO using Eu_2O_3. The experimental procedure was kept same. In Eu doped SYO samples, Eu_2O_3 was taken in addition to $SrCO_3$ and Y_2O_3 in a stoichiometric ratio according to the formula $SrY_{(2-x)}O_4:xEu^{3+}$ (x= 0.01, 0.03, 0.05, 0.07, 0.09, and 0.11). All the synthesis steps followed same for the Eu doped SYO samples as aforementioned. It was found that maximum intensity of luminescence was found for 9 mol% of europium ions in the host lattice. The co-doping of Ti was done by taking stoichiometric amount of TiO_2, Eu_2O_3, $SrCO_3$ and Y_2O_3 according to the formula $SrY_{1.91-y}Eu_{0.09}O_4$ (y= 0.01, 0.02, 0.03, 0.04, 0.05 and 0.06). The same synthesis steps were followed to synthesize co-doped samples. The final end products of undoped, doped and co-doped SYO samples were ground to make fine powder and then used for further characterization to study structural, and optical properties.

4.3. Characterization Techniques

(a) X-Ray Diffraction (XRD): XRD studies were carried out to understand the crystal structure, phase purity, and crystallite size using Panalytical X'Pert Pro XRD diffractometer using Cu-Kα radiation with in-built Ni filter operating at 45 kV. The XRD data was recorded in a wide range of Bragg angles, $10 \leq \theta \leq 80°$. The XRD patterns were analysed for phase identification using X'Pert High Score software using ICDD database.

(b) Photoluminescence (PL): The emission and excitation spectra of the samples were recorded using a fluorescent spectrometer (Agilent Technologies- Model Cary Eclipse) equipped with Xenon lamp. A fixed amount (0.1 gram) of all the doped samples was used for recording the spectra. The slit width of excitation and emission slit were set at 2.5 and 2.5 nm.

(c) Fourier Transform Infrared Spectroscopy (FTIR): The FTIR spectra of the samples were recorded using Perkin-Elmer-Spectrum RX-IFTIR spectrometer in the range 400 – 4000 cm^{-1} range using KBr pellet technique.

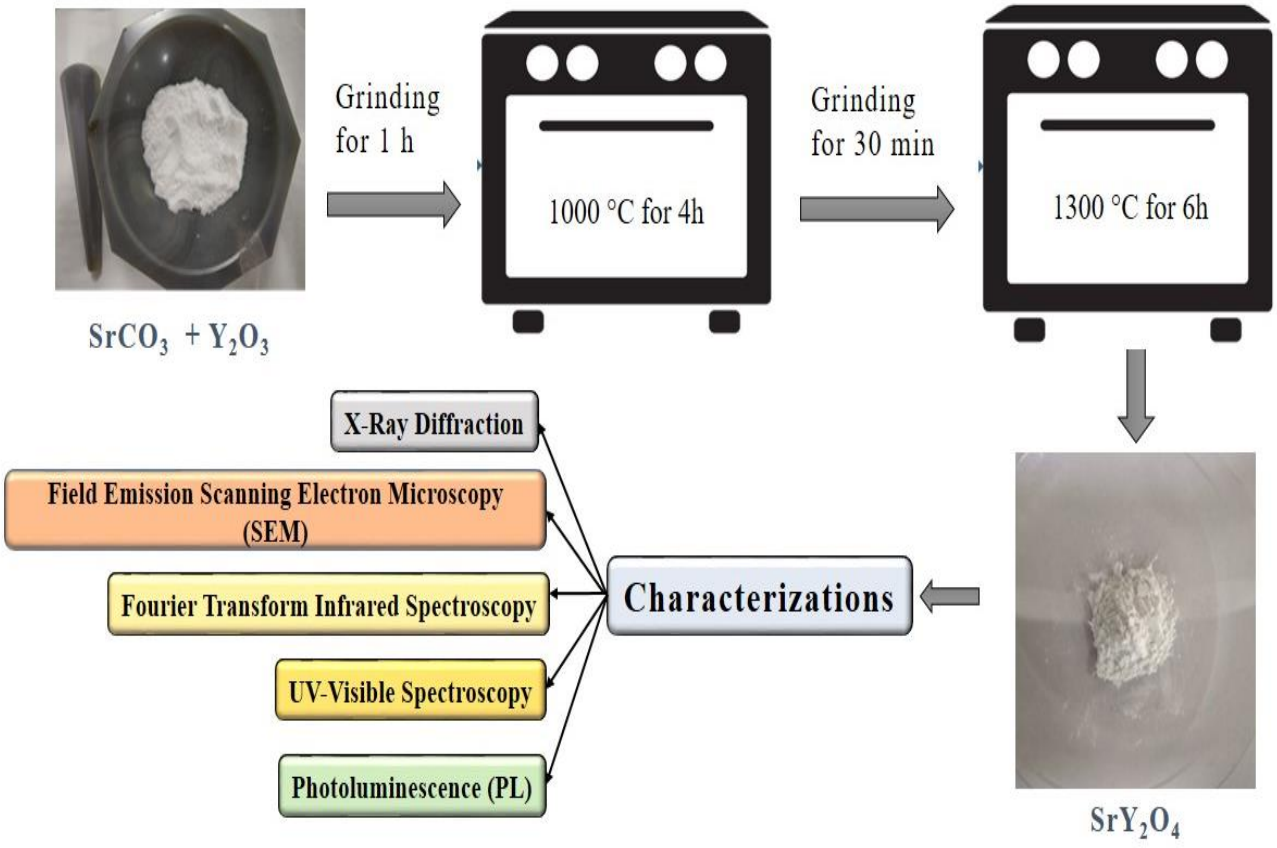

Figure 4.1: Schematic representation of synthesis and characterization of un-doped SrY_2O_4 phosphors.

CHAPTER 5
RESULTS AND DISCUSSIONS

5.1. X-Ray diffraction (XRD)

Fig. 5.1 represents the X-Ray diffractograms of undoped SrY_2O_4 (SYO) samples heat treated at 1000 and 1300 °C. It is observed that XRD patterns of undoped SYO synthesized at 1000 °C consist of peaks corresponding to orthorhombic SYO and cubic-Y_2O_3 phase, when matched with International Centre for Diffraction Data (ICDD) card number 00-032-1272 (SYO) and 00-076-0151 (Y_2O_3), respectively. The peaks around 29.20 ° and 48.57 ° correspond to Y_2O_3 phase present in the samples.

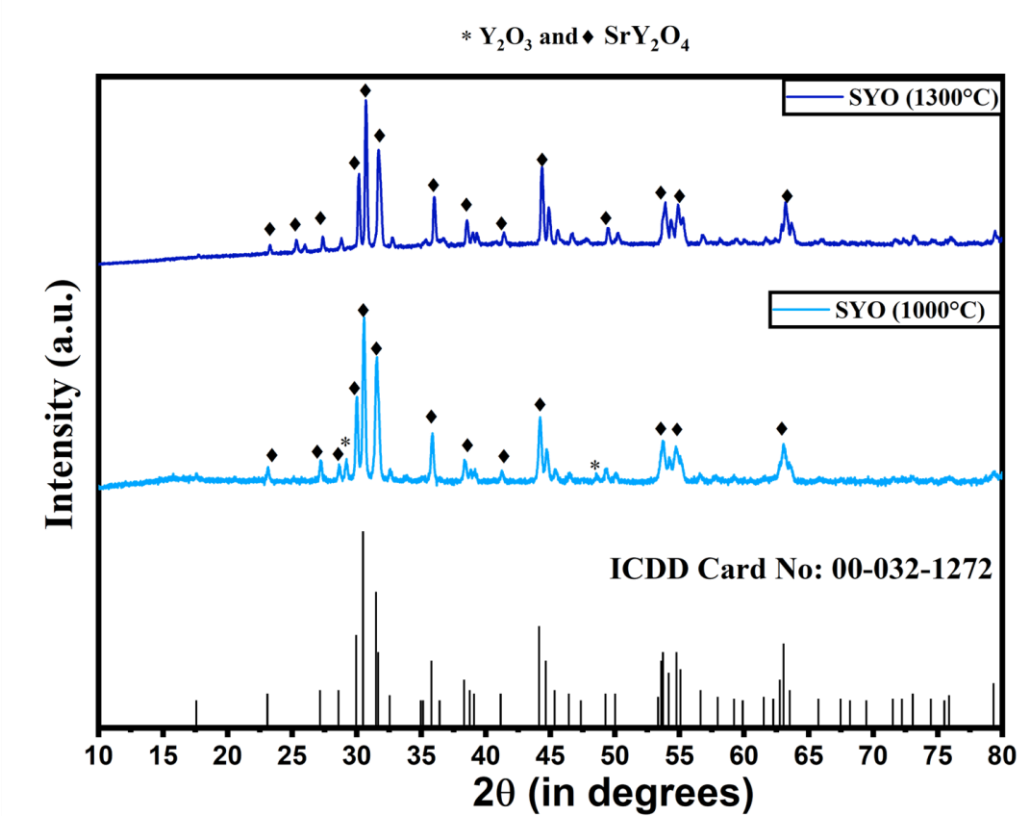

Figure 5.1: X-Ray diffraction pattern of un-doped SrY_2O_4 phosphors calcined at 1000 and 1300 °C.

The SYO sample synthesized at 1300 °C consists of high intense, sharp and crystalline peaks attributed to pure orthorhombic SYO phase (ICDD: 00-032-1272) having *Pnam* (62) group symmetry. In such samples, no other impure phase corresponding to initial precursors or Y_2O_3 and SrO are found. **Fig. 5.2** represents the XRD patterns of europium doped (1, 3, 5, 7, 9 and 11 mol %) SYO samples calcined at 1300 °C. Eu doped SYO samples are well matched with the ICDD card no. 00-032-1272.

It is observed that incorporation of Eu^{3+} ions in SrY_2O_4 had no effect on the phase change of the host lattice. No secondary phase corresponding to Eu_2O_3 is observed in the doped samples. It indicates that the doped ions are well incorporated into the various sites of the host lattice.

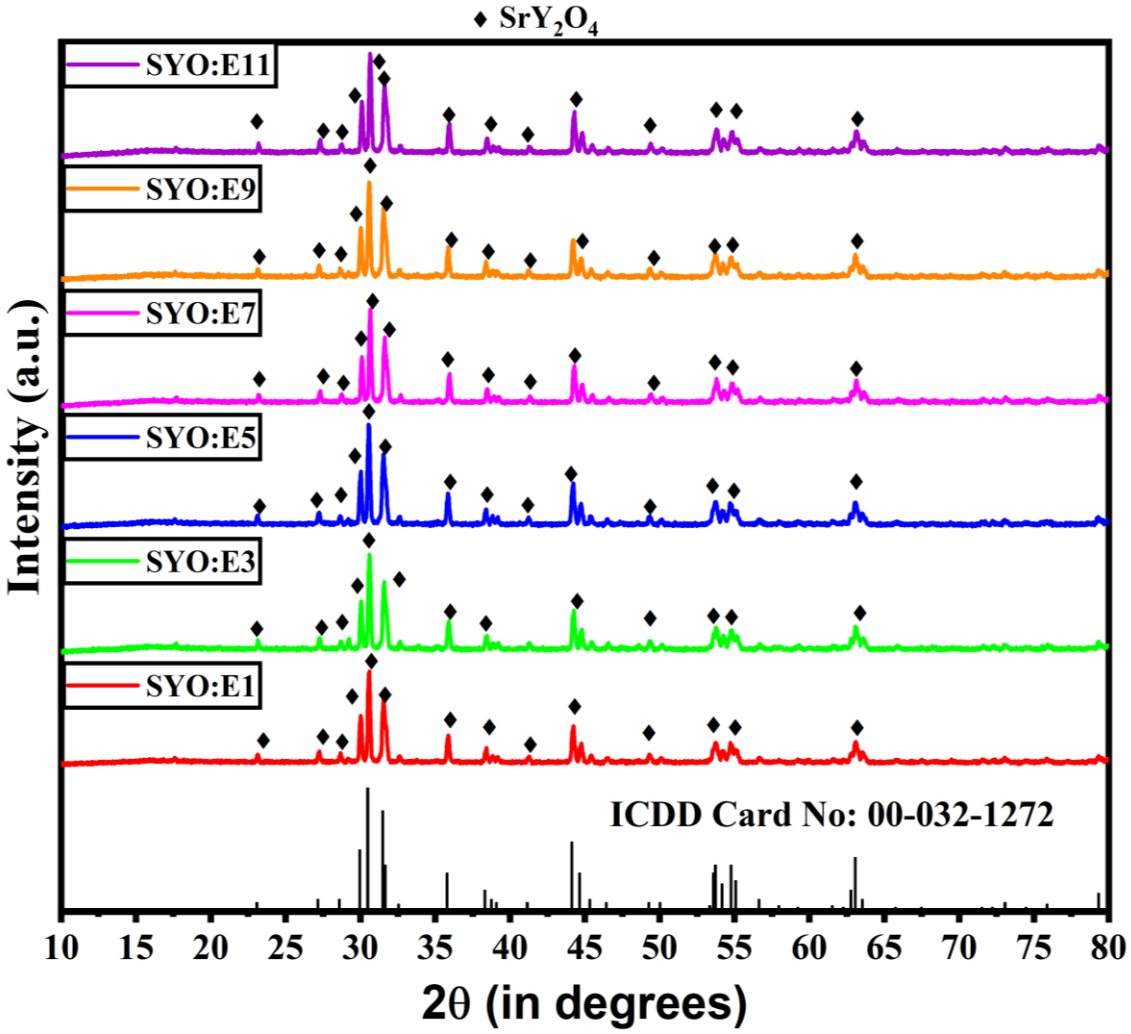

Figure 5.2: X-Ray diffraction patterns of Eu^{3+} activated SrY_2O_4 phosphors.

The average crystallite size (D) of the samples is calculated via Debye Scherrer formula [1]:

$$D = \frac{0.9\,\lambda}{\beta\,\cos\theta} \qquad (5.1)$$

where, λ is the wavelength of incident X-rays (0.15406 nm), θ is the angle of diffraction of the observed peak and β is the full width at half maximum (FWHM). β used in equation 1 is highly dependent on both instrumental and sample effects. β is corrected using standard sample of Si and determined using the following equation [2]:

$$\beta = \{(\beta_{experimental})^2 - (\beta_{instrumental})^2\}^{1/2} \quad (5.2)$$

The calculated values of the crystallite size of all the samples is tabulated in **Table 5.1**. It is observed that the average crystallite size of the doped samples is more than the undoped samples. This is due to the fact that ionic radii (r) of the europium ions (r = 0.95 Å) is greater that the yttrium ions (r = 0.89 Å) [3], which leads to the increase in the crystallite size.

Table 5.1. Crystallite size of Eu doped and undoped SrY_2O_4.

Sample ID	Dopant Concentration (in mol%)	2θ (degree)	Crystallite size (nm)
SYO	0	30.73	45.88
SYO:E1	1	30.57	47.95
SYO:E3	3	30.60	48.37
SYO:E5	5	30.56	47.27
SYO:E7	7	30.65	51.20
SYO:E9	9	30.58	47.38
SYO:E11	11	30.65	48.48

5.2. Fourier transform infrared (FTIR) spectroscopy

Fig. 5.3 (a) and (b) represent the FTIR spectra of un-doped and Eu^{3+} doped SrY_2O_4 phosphors in the range 400-4000 cm^{-1} and 450-700 cm^{-1}, respectively. The intense absorption band around 3430 cm^{-1} corresponds to O-H stretching vibration, which is due to the absorption of water molecules from the atmosphere. The bands lying in the range 1473-1634 cm^{-1} are attributed to the presence of Sr-O bond. The peaks ranging from 450-700 cm^{-1} are the characteristics of Y-O vibrations. The O-Y-O group vibrations are observed around 606 cm^{-1} [4,5]. The presence of all these bands confirm the formation of SrY_2O_4 phosphors.

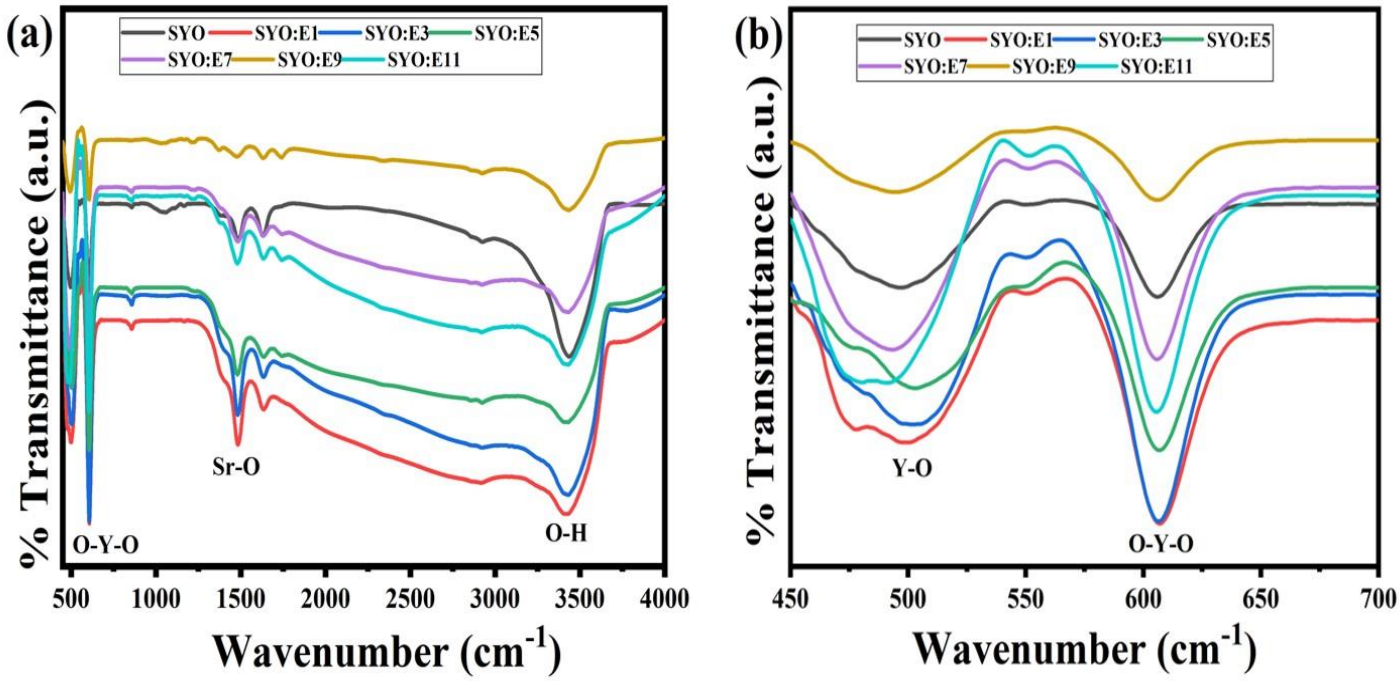

Figure 5.3: FTIR spectra of SrY_2O_4 doped with Eu^{3+} at different concentrations (a) in the range 400-400 cm^{-1} and (b) in the range 450-750 cm^{-1}.

5.3. Photoluminescence (PL) studies

The photoluminescence excitation (PLE) spectra of 9 mol% Eu activated SrY_2O_4 (SYO) is shown in **Fig. 5.4**. The excitation spectra are recorded at 611 nm wavelength in the range 200-500 nm and a broad band is observed around 227 nm. The broad excitation band present is called charge transfer band (CTB). The CTB is due to the charge transfer between partially filled 4f orbital of the Eu^{3+} ion and the completely filled 2p orbital of the O^{2-} ion. Also, the position of CTB depends on the host lattice [6]. The broad and intense excitation band is observed in the deep ultraviolet (UV) range. Thus, Eu activated SYO phosphors are UV excited phosphors.

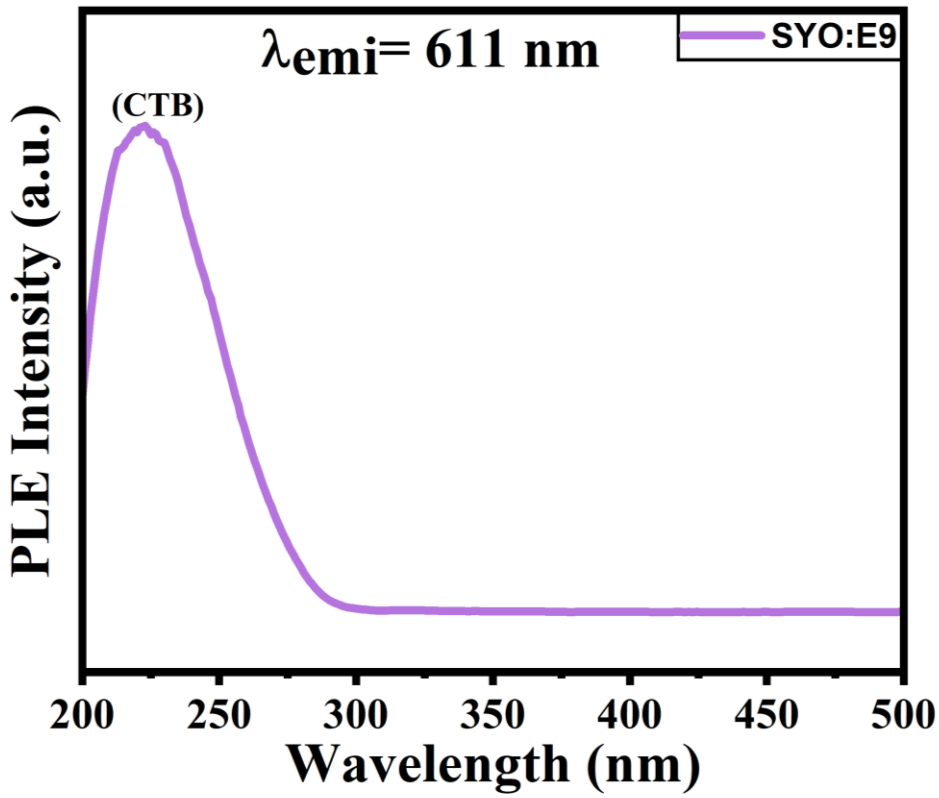

Figure 5.4: PL excitation spectra of 9 mol % Eu doped SrY_2O_4.

The emission spectra of $SrY_2O_4:Eu^{3+}$ under 227 nm excitation are recorded in the range 550-750 nm, as shown in **Fig. 5.5**. The emission peaks are observed around 580, 587, 592, 597, 611, 625, 652, 656 and 709, 712 nm. All the emission peaks are corresponding to the europium ion transitions. The emission spectra reveal that the emission bands are originated from the relaxation of $^5D_0$ excited state to $^7F_1$, $^7F_2$, $^7F_3$ and $^7F_4$ states [7]. The moderate intense emission band at 580 nm is occurring due to $^5D_0 \rightarrow {}^7F_0$ transition of Eu^{3+} ion. The emission peaks centered at 587, 592 and 597 nm are due to $^5D_0 \rightarrow {}^7F_1$ transition. The strongest emission peak is observed due to $^5D_0 \rightarrow {}^7F_2$ transition around 611 nm.

There is another peak at 625 nm occurring due to $^5D_0 \rightarrow {}^7F_2$ transition. This splitting of $^5D_0 \rightarrow {}^7F_1$ and $^5D_0 \rightarrow {}^7F_2$ peaks is attributed to 'Stark splitting' of $^7F_1$ and $^7F_2$ state respectively. The $^7F_1$ transitions are identified as magnetic dipole transitions and exhibit splitting sue to the ligand field experienced by them. The transitions corresponding to $^5D_0 \rightarrow {}^7F_2$ are identified as electric dipole and are highly sensitive to the local domain of Eu^{3+} in the host matrix, therefore the splitting is attributed to Eu^{3+} ions occupying two

different sites in the SYO host lattice [8]. The weak emission bands observed at 652, 656 nm and 709, 712 nm are due to $^5D_0 \rightarrow {}^7F_3$ and $^5D_0 \rightarrow {}^7F_4$ transitions, respectively.

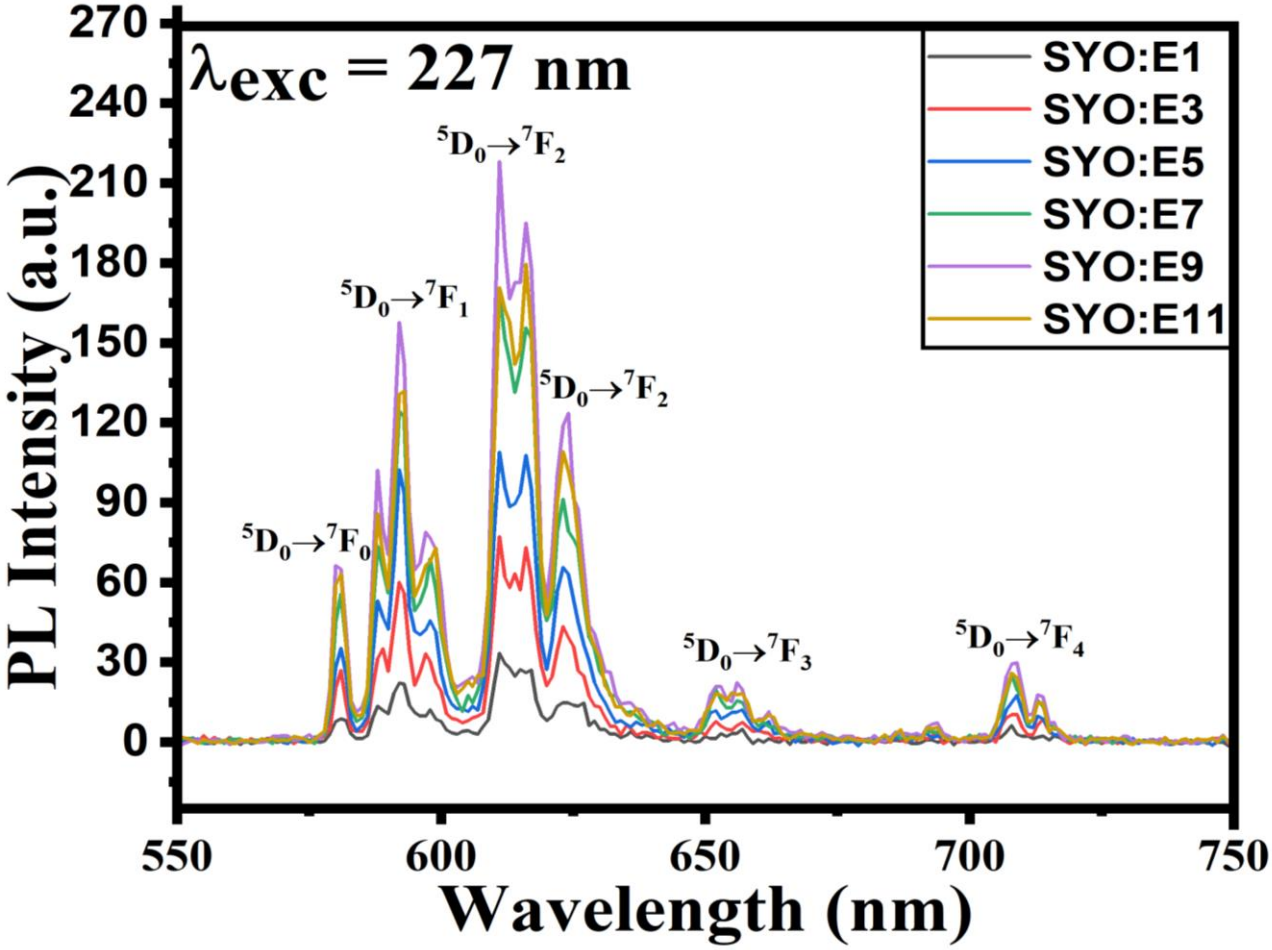

Figure 5.5: PL emission spectra of Eu doped SrY_2O_4 phosphors.

The variation in the intensity of the emission peak centered at 582, 592, 611 and 625 nm with varying concentration of Eu in SYO is shown **Fig. 5.6**. It is observed that with increase in Eu^{3+} concentration, PL emission intensity first increases and then decreases beyond 9 mol% Eu^{3+} ions. The decrease in PL intensity beyond 9 mol% of Eu concentration in SYO occurs as a consequence of quenching effect [9]. Thus, the maximum emission intensity is found for 9 mol% Eu^{3+} ions in SrY_2O_4 host lattice.

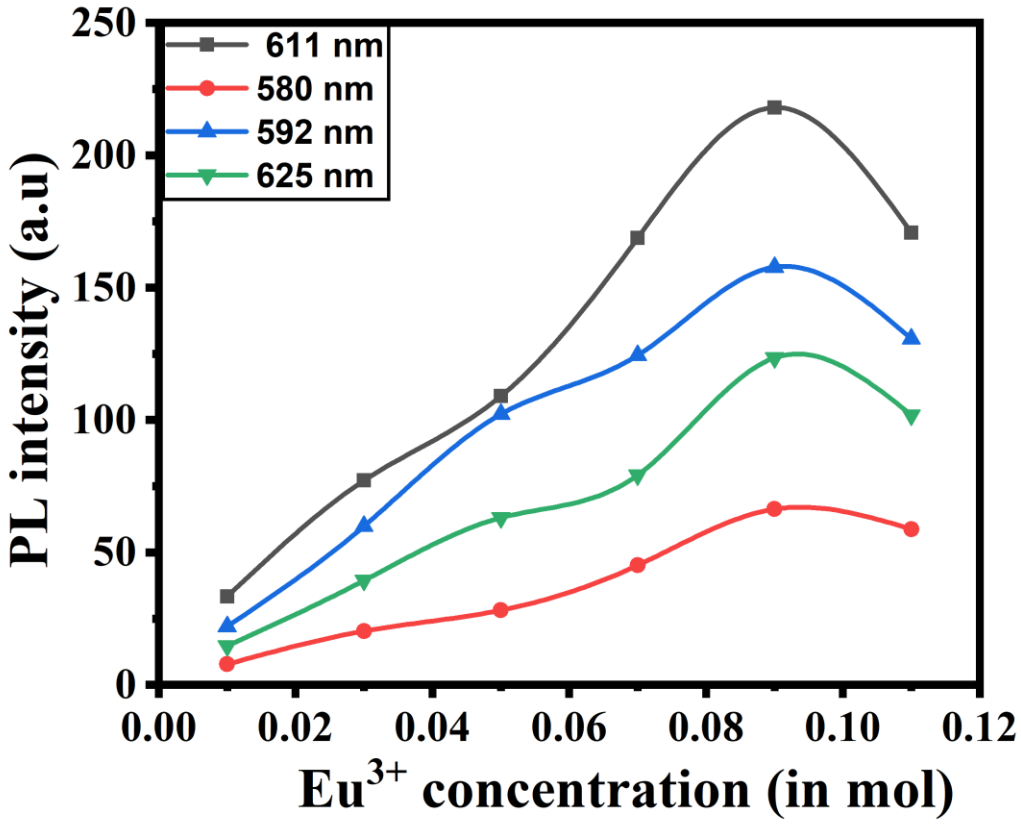

Figure 5.6: Variation in emission intensity of peak centered at λ= 580, 592, 611 and 625 nm with changing Eu^{3+} concentration.

There are several reasons of concentration quenching like non-radiative energy transfer between the europium ions. As the concentration of Eu^{3+} ions increases, the minimum distance between the Eu^{3+} ions decreases and it leads to the non-radiative energy transfer [10]. Blasse's equation can be used to determine the minimum distance (R_C), which is known as the critical distance. According to this theory, if the R_C value is 5 Å or less, exchange interaction leads to non-radiative transfer and the value of R_C greater than 5 Å, leads to multipole-multipole interactions [11]. According to Blasse's equation, the critical distance R_C is given by the formula:

$$R_C = 2\left[\frac{3V}{4\pi N x_C}\right]^{1/3} \quad (5.3)$$

Where, V is the volume of unit cell, x_C refers to the critical doping concentration and N is the number of available sites for activator in the host. For SrY_2O_4:9 mol% Eu^{3+}, V=409.37 $Å^3$, x_C=0.09 and N=8; results in critical distance of 10.28 Å. It implies that the

multipolar interactions are the major cause for the concentration quenching in the host lattice.

The sort of multipolar interaction involved in the energy transfer phenomenon can be determined using Dexter and Schulman's theory [12]. According to this theory, the photoluminescence intensity (I) per activator is given by:

$$\frac{I}{x} = \frac{K}{1+\beta(x)^{Q/3}} \tag{5.4}$$

where, K and β are constants related with a particular interaction and x is the concentration of activator ions. The type of interaction is determined by finding value of Q which is calculated using slope of the graph (-Q/3) plotted between log(I/x) verses log(x), as shown in **Fig. 5.7**. Q can take values 6, 8 or 10 and less than 6 corresponding to the dipole-dipole, dipole-quadrupole, quadrupole-quadrupole interactions, and charge transfer mechanism, respectively.

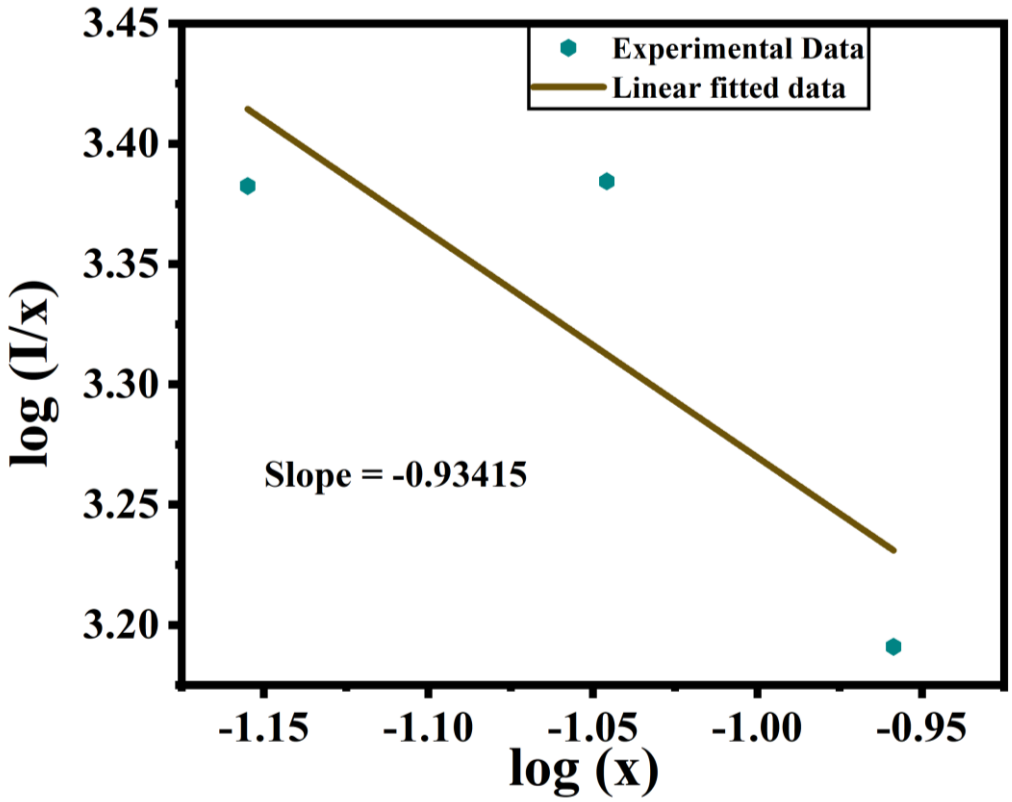

Fig. 5.7. Plot of log(I/x) verses log(x) for $SrY_2O_4:Eu^{3+}$ at 227 nm excitation.

For the present case, the slope of the graph for 227 nm excitation is found to be -0.93415. This leads the Q value to be 2.802, which is less than 6, which implies that the energy transfer among the nearest neighbouring ions is the primary cause of concentration

quenching. The energy level diagram of excitation and emission spectra of Eu doped SYO phosphors corresponding to different transitions is shown in **Fig. 5.8.**

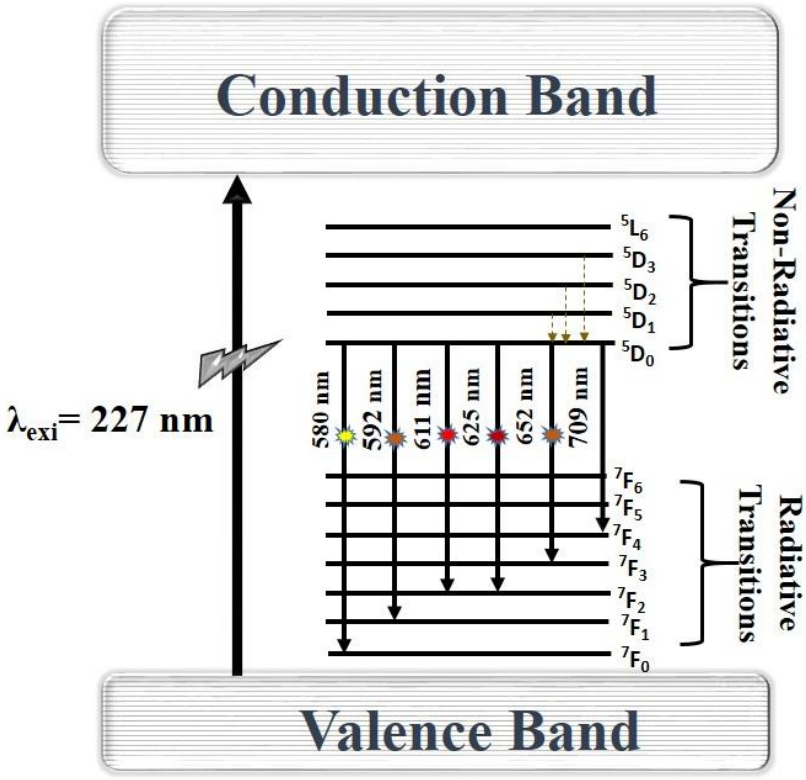

Figure 5.8: Energy level diagram of SrY_2O_4:Eu.

The emission spectra of the as-synthesized phosphors are further analyzed via plotting the CIE (International Commission on Illumination) diagram. The CIE coordinates are calculated from the emission spectra using a CIE color calculator program in MTLAB 9.1 (version R2016b). **Fig. 5.9** illustrates the CIE diagram of SrY_2O_4:xEu^{3+} (x= 0.01, 0.03, 0.05, 0.07, 0.09 and 0.11). The computed CIE coordinates of the as-synthesized phosphors fall in the red region. According to National Television Standard Committee (NTSC), the ideal value of coordinates for red color are x = 0.67, and y = 0.33 [13]. The calculated CIE coordinates of Europium doped phosphors lie close to the red region. Thus, these phosphors have potential to be utilized in optoelectronic devices for red light emission.

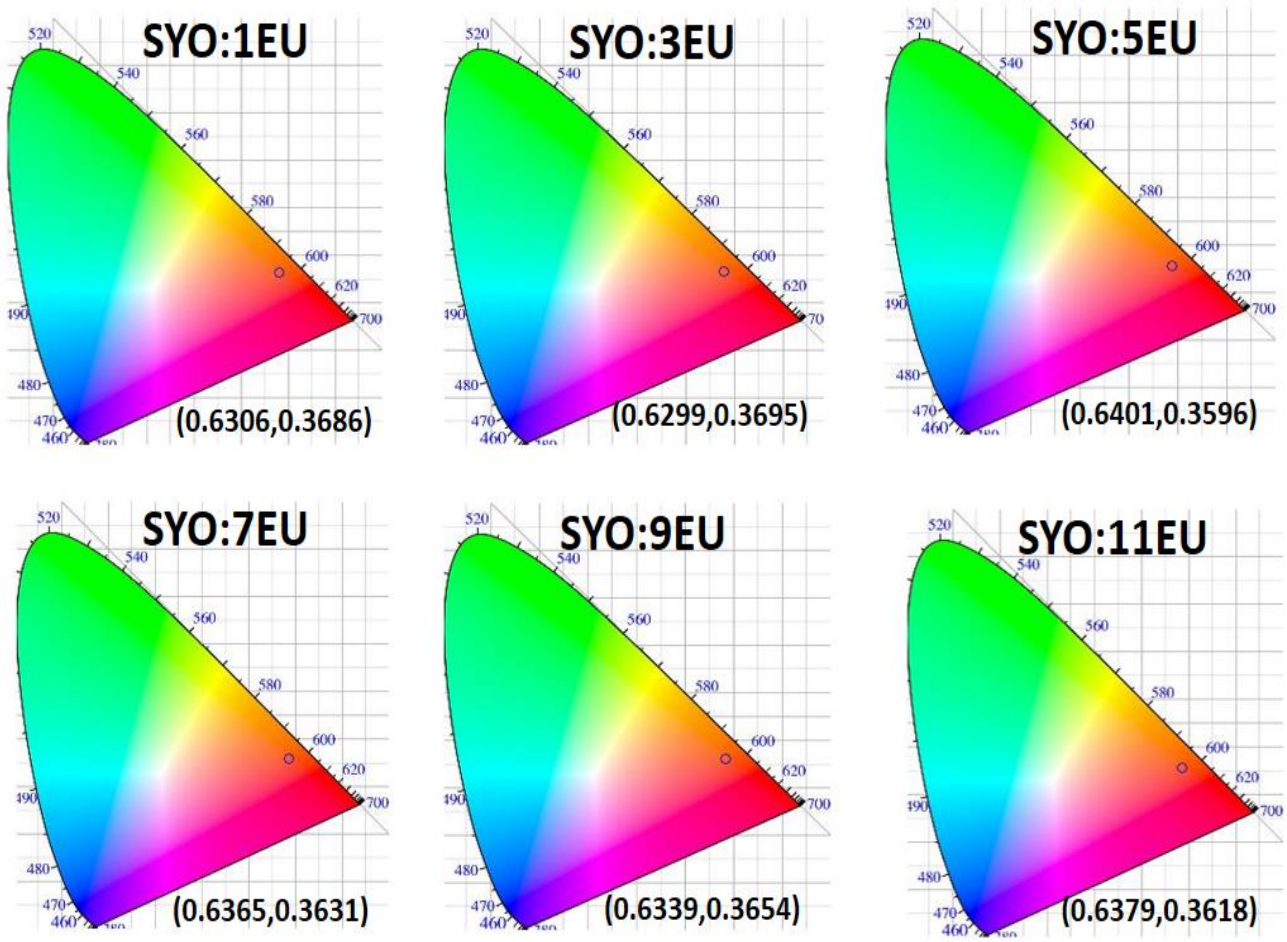

Figure 5.9: CIE coordinates diagram of $SrY_2O_4:xEu^{3+}$(x = 0.01, 0.03, 0.05, 0.07, 0.09 and 0.11)

Further, effect of co-doping of titanium is studied in the optimized sample, i.e., 9mol% Eu doped SYO sample at which maximum PL intensity is observed. The concentration of titanium is varied from 1 to 5 mol%. The emission spectra are recorded under 227 nm excitation in the range 550-800 nm, as shown in **Fig. 5.10.** The major emission peaks are observed around 580, 587, 592, 598, 611, 616, 623, 652, 656, 709, and 712 nm. All the emission peaks are corresponding to the transitions from $^5D_0$-$^7F_{1,2,3,4}$ states of europium ion. The most intense and prominent emission peak is observed due to $^5D_0 \rightarrow {}^7F_2$ transition around 616 nm. It is observed that maximum intensity peak for the Eu doped SYO samples is around 611 nm, while for co-doped samples, it gets red shifted to 616 nm. This indicates that after co-doping samples exhibited more red emission.

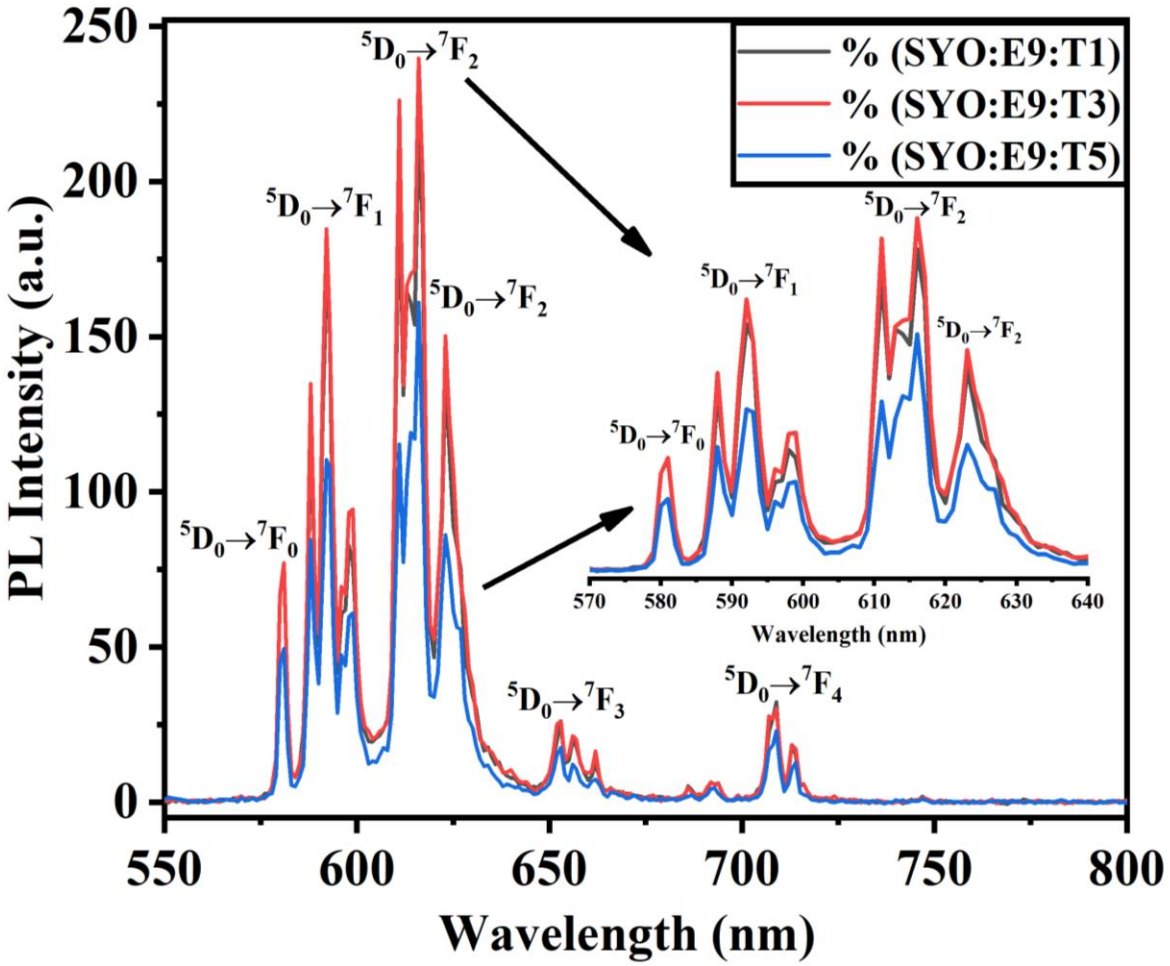

Figure 5.10: PL emission spectra of Ti doped $SrY_2O_4:Eu^{3+}$ phosphors.

The variation in the PL intensity of the emission peaks centered at 580, 592, 616 and 623 nm with varying concentration of Ti in SYO for a fixed 9 mol % of Eu^{3+} ion is shown **Fig. 5.11**. It is observed that with increase in titanium concentration, PL emission intensity increases and reaches its maximum when the co-doping concentration is found to be 3 mol %. With increase in the doping concentration of Ti ions beyond 3 mol% PL intensity decreases due to concentration quenching. This quenching is attributed to presence of excessive doping of Ti ions in the Eu doped SYO phosphors which leads to cross relaxation of neighbouring Ti ions. The emission intensity of co-doped samples is more than that of doped samples because the energy transfer between co-doped ions and Eu^{3+} ions leading in increase in intensity of radiative emission.

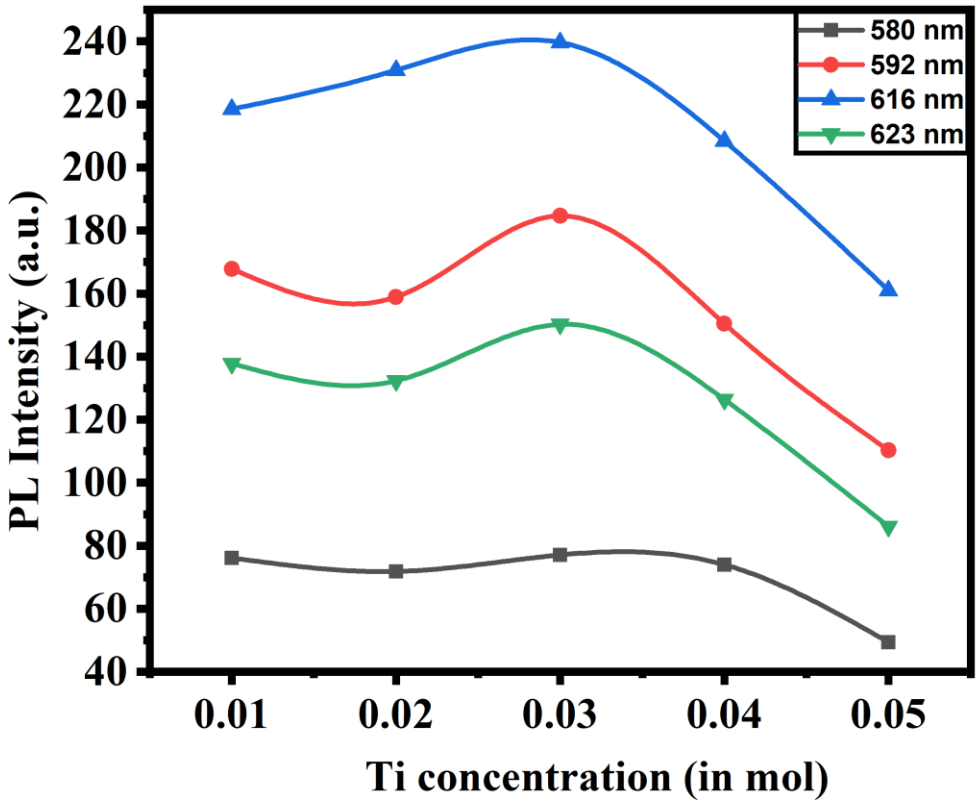

Figure 5.11: Variation in emission intensity of peak at λ= 580, 592, 611 and 625 nm with changing Eu^{3+} concentration.

Fig. 5.12 illustrates the CIE diagram of SrY_2O_4:9 %Eu^{3+}/xTi (x= 0.01, 0.02, 0.03, 0.04 and 0.05). The computed CIE coordinates of the as-synthesized phosphors fall very close to the red region. The ideal value of coordinates for red color according to National Television Standard Committee (NTSC), are x = 0.67, and y = 0.33. The calculated chromaticity coordinates for Ti co-doped samples are (0.637,0.362), (0.636,0.363), (0.639,0.360), (0.638,0.361) and (0.635,0.364) for SrY_2O_4:9Eu^{3+}/1Ti, SrY_2O_4:9Eu^{3+}/2Ti, SrY_2O_4:9Eu^{3+}/3Ti, SrY_2O_4:9Eu^{3+}/4Ti and SrY_2O_4:9Eu^{3+}/5Ti respectively. Thus, due to enhancement of PL emission intensity and more red shifted emission wavelength the co-dopes samples found potential applications in various optoelectronic devices.

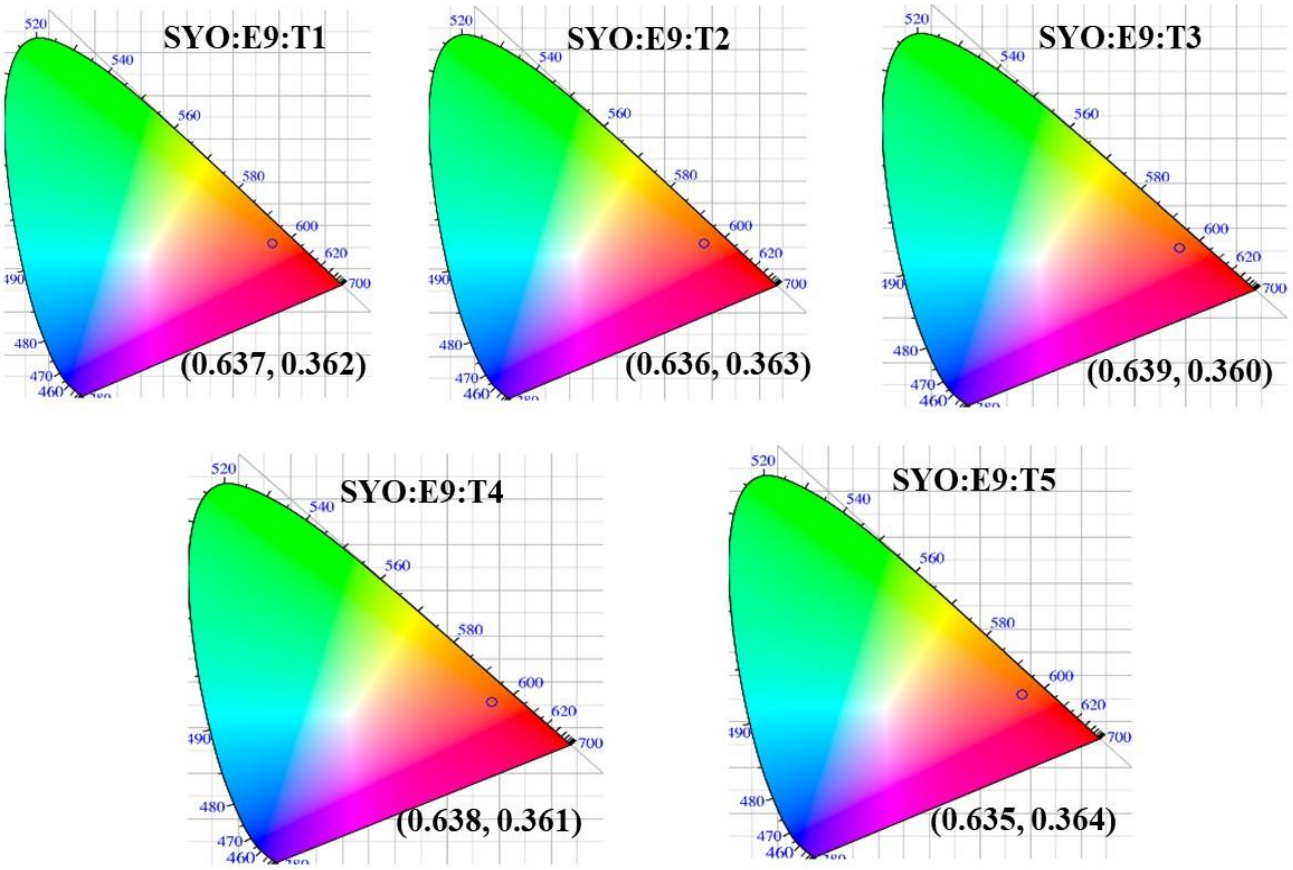

Figure 5.12: CIE coordinates diagram of SrY_2O_4:9 %Eu^{3+}/x Ti(x = 0.01, 0.02, 0.03, 0.04 and 0.05)

REFERENCES

1. Singh V, Swapna K, Kaur S, Rao A.S, Rao J.L, (2020), Narrow-Band UVB-Emitting Gd-Doped SrY_2O_4 Phosphors. J Electron Mater 49:3025–3030.
2. Kaur N, Mir R.A, Pandey O.P, (2019), Electrochemical and optical studies of facile synthesized molybdenum disulphide (MoS_2) nano structures. J Alloys Compd 782:119–131.
3. Kolesnikov I.E, Povolotskiy A.V, Mamonova D.V, Lahderanta E, Manshina A.A, Mikhailov M.D, (2016), Photoluminescence properties of Eu^{3+} ions in yttrium oxide nanoparticles: Defect: Vs. Normal sites. RSC Adv 6:76533–76541.
4. Ghorpade S.P, Hari Krishna R, Melavanki R.M, Dubey V. Patil N.R, (2020), Effect of Eu^{3+} on optical and energy bandgap of SrY_2O_4 nanophosphors for FED applications. Optik (Stuttg) 208:164533.
5. Dubey V, Kaur J, Agrawal S, (2015), Effect of europium doping levels on photoluminescence and thermoluminescence of strontium yttrium oxide phosphor. Mater Sci Semicond Process 31:27–37.
6. Singh D, Tanwar V, Bhagwan S, Nishal V, Sheoran S, Kadyan S, Samantilleke A.P, Kadyan P.S, (2015), Synthesis and Optical Characterization of Europium Doped MY_2O_4 (M = Mg, Ca, and Sr) Nanophosphors for Solid State Lightening Applications. Indian J Mater Sci 2015:1–8.
7. Li Y, Hong G, (2007), Synthesis and luminescence properties of nanocrystalline Gd_2O_3:Eu^{3+} by combustion process. J Lumin 124:297–301.
8. Som T, Karmakar B, (2010), Optical properties of Eu^{3+}-doped antimony-oxide-based low phonon disordered matrices. J Phys Condens. Matter 22.
9. Taikar D.R, (2018), Synthesis and luminescence property of SrY_2O_4:M (M = Eu^{3+}, Tb^{3+}, Sm^{3+}, Ce^{3+}, Bi^{3+}) phosphors. J Lumin 204:24–29.
10. Blasse G, (1986), Energy transfer between inequivalent Eu^{2+} ions. J Solid State Chem 62:207–211.
11. Priya R, Khurana I, Pandey O.P, (2020), Synthesis of intense red light-emitting β-Ca_2SiO_4:Eu^{3+} phosphors for near UV-excited light-emitting diodes utilizing agro-food waste materials. J Mater Sci Mater Electron 31:1912–1928.
12. Liu Y, Liu G, Wang J, (2015), Multicolor photoluminescence and energy transfer properties of dysprosium and europium-doped Gd_2O_3 phosphors. J Alloys and compounds 649:96-103.
13. Priya R, Negi A, Singla S, Pandey O.P, (2020), Luminescent studies of Eu doped $ZnAl_2O_4$ spinels synthesized by low-temperature combustion route. Optik (Stuttg) 204:164-173.

CHAPTER 6
CONCLUSION AND FUTURE SCOPE

6.1. Conclusion

In the present work, structural and photoluminescent studies of Eu doped SrY_2O_4 (SYO) have been conducted. All the undoped SYO, Eu doped SYO, Ti co-doped SYO:Eu samples have been successfully synthesized via solid-state method. The pure phase, crystalline SYO was formed at 1300 ℃, which was confirmed by the XRD results. The phase of synthesized SYO samples was orthorhombic with *Pnam* space group. The average crystallite size of the doped samples was found to be more than the undoped samples. This is owing to the fact that size of europium ions is more than the yttrium ions. FTIR results also confirmed the formation of pure SYO samples. In FTIR spectra, the vibrations corresponding to Y-O, O-Y-O and Sr-O were observed. The concentration of the Eu^{3+} ions in SYO lattice was varied from 1 to 11 mol%. In the excitation spectra, the broad band was observed around 227 nm, thus implying that synthesized phosphors are UV excited phosphors. Further, emission spectra consisted of several peaks corresponding to the transitions of Eu^{3+} ions. The maximum PL intensity was observed at 9 mol% of Eu^{3+} ions in the SYO lattice. For the Ti co-doped SYO:Eu samples maximum PL intensity was observed at 616 nm for 3 mol % concentration of Ti. The CIE of both Eu doped and Ti co-doped phosphors lie in the red region. The as-synthesized samples find potential applications in the optoelectronic and display devices.

6.2. Future Scope

In the present work, SrY_2O_4 phosphors doped with europium and co-doped with titanium have been synthesized. The structural and photoluminescent properties have been studied in detail. There are still further research possibilities are left to carry out in future. The other rare-earth such as Dy^{3+}, Pr^{3+}, Sm^{3+}, Tb^{3+}, Er^{3+}, Pr^{3+}, Gd^{3+}, and Ho^{3+} etc. can be used as activator ions in order to get emissions of desired colors for various applications. Also, the other transitions elements such as Mn, Sc, Co, Mo, V, Mo, etc. can be utilized as sensitizers to enhance and improve the emission characteristics of doped SrY_2O_4 phosphors. Apart from the solid-state reaction method, other synthesis routes and reaction conditions can be optimized to get different nanostructures of SrY_2O_4 phosphors.

Smriti

Turnitin Originality Report

Processed on: 2021年06月27日 14:35 +0530
ID: 1612674806
Word Count: 4807
Submitted: 1

Similarity Index	Similarity by Source
14%	Internet Sources: 3% Publications: 11% Student Papers: 4%

Smriti Thesis By Smriti Smriti

2% match (publications)
Ruby Priya, O.P. Pandey, Sanjay J. Dhoble. "Review on the synthesis, structural and photo-physical properties of Gd2O3 phosphors for various luminescent applications", Optics & Laser Technology, 2021

1% match (student papers from 20-Jun-2019)
Submitted to Thapar University, Patiala on 2019-06-20

1% match (publications)
Ruby Priya, Ishita Khurana, Om Prakash Pandey. "Synthesis of intense red light-emitting β-Ca2SiO4:Eu3+ phosphors for near UV-excited light-emitting diodes utilizing agro-food waste materials", Journal of Materials Science: Materials in Electronics, 2019

1% match (publications)
Yan Liu, Guixia Liu, Jinxian Wang, Xiangting Dong, Wensheng Yu. " Single-Component and Warm-White-Emitting Phosphor NaGd(WO) :Tm , Dy , Eu : Synthesis, Luminescence, Energy Transfer, and Tunable Color ", Inorganic Chemistry, 2014

1% match (publications)
Ruby Priya, Sandeep Kaur, Utkarsh Sharma, O. P. Pandey, Sanjay J. Dhoble. "A review on recent progress in rare earth and transition metals activated SrY2O4 phosphors", Journal of Materials Science: Materials in Electronics, 2020

1% match (publications)
Eluri Pavitra, Ganji Seeta Rama Raju, Ganji Lakshmi Varaprasad, Nilesh R. Chodankar et al. "Desired warm white light emission from a highly photostable and single-component Gd2TiO5:Dy3+/Eu3+ nanophosphors for indoor illuminations", Journal of Alloys and Compounds, 2021

< 1% match (student papers from 18-Jul-2016)
Submitted to Thapar University, Patiala on 2016-07-18

< 1% match (student papers from 06-Jul-2019)
Submitted to Thapar University, Patiala on 2019-07-06

< 1% match (Internet from 04-Nov-2020)
https://worldwidescience.org/topicpages/b/brilliant+sm+eu.html

< 1% match (Internet from 08-Oct-2020)
https://worldwidescience.org/topicpages/c/ce+tehdasoloissa+tapahtuva.html